Chapter 6
Earth Rotation

Florian Seitz and Harald Schuh

Contents

The rotation of the Earth varies continuously. Its rotation axis changes its orientation with respect to both a space-fixed and an Earth-fixed reference system, and the angular velocity of the rotation fluctuates with time. The knowledge and therewith the continuous observation of Earth rotation variations is important for various reasons. It is fundamental for the realisation of time systems, the accurate determination of reference frames and precise navigation by providing the link between an Earth-fixed and a space-fixed coordinate system. Moreover, time series of Earth rotation parameters are of great interest for various disciplines of geosciences and astronomy since their changes are related to gravitational and geodynamic processes in the Earth system. In this way, Earth rotation monitoring contributes significantly to the understanding of the dynamics of the Earth system and the interactions between its individual components, e.g. the exchange of angular momentum between atmosphere, ocean and solid Earth, or the coupling mechanism between the Earth's core and mantle. Today the metrological basis for this highly interdisciplinary research is provided by precise space geodetic techniques such as Very Long

F. Seitz (✉)
Earth Oriented Space Science and Technology, Technische Universität München (TUM), Arcisstr. 21, D-80333 Munich, Munich, Germany
e-mail: seitz@bv.tum.de

G. Xu (ed.), *Sciences of Geodesy – I*, DOI 10.1007/978-3-642-11741-1_6,

Baseline Interferometry (VLBI), Satellite/Lunar Laser Ranging (SLR/LLR), Global Navigation Satellite Systems (GNSS) and ring laser gyroscopes.

6.1 Reference Systems

Generally speaking the rotation of the Earth can be interpreted as a change of the orientation of an Earth-fixed reference system $\mathcal{H}$ relative to a space-fixed reference system $\mathcal{I}$.

The rotation vector of the Earth ω changes its orientation and its absolute value with respect to either system. Independent of the coordinate system, the rotation vector is the vector that provides the direction of the instantaneous rotation axis. Its absolute value equals the instantaneous angular velocity of Earth rotation. The temporal variations of the Earth rotation vector in the space-fixed reference system are known as precession and nutation. Both are caused by lunisolar gravitational torques which can be described as functions of time by series expansions with high accuracy. The effects of precession and nutation have been known for centuries from astronomical observations. The change of the direction of the Earth rotation vector with respect to an Earth-fixed reference system is referred to as polar motion and was not observed before the end of the nineteenth century. Different to precession and nutation, polar motion and the variation of the Earth's angular velocity are not easily predictable since they are affected by a multitude of irregular geodynamic processes.

According to a fundamental theorem of rotational dynamics, the temporal derivative of the rotation vector of a rotating body is equal with regard to a body-fixed and a space-fixed reference system. The temporal derivative $\frac{\mathrm{d}x}{\mathrm{d}t}$ of an arbitrary vector x with respect to a body-fixed system and its temporal derivative $\frac{\mathrm{D}x}{\mathrm{D}t}$ with respect to a space-fixed system are related by

$$\frac{\mathrm{D}x}{\mathrm{D}t} = \frac{\mathrm{d}x}{\mathrm{d}t} + \omega \times x \,. \tag{1}$$

If the Earth rotation vector ω is introduced instead of x, the equation turns into

$$\frac{\mathrm{D}\omega}{\mathrm{D}t} = \frac{\mathrm{d}\omega}{\mathrm{d}t} + \omega \times \omega = \frac{\mathrm{d}\omega}{\mathrm{d}t} \,. \tag{2}$$

The equality of the derivatives means that the derivative of both the orientation of the rotation vector and its absolute value is identical in the two systems. Consequently the variations of the orientation of the Earth rotation axis in the space-fixed and in the Earth-fixed reference system are not independent of each other. The relation between the coordinates of the Earth rotation vector with regard to a space-fixed or Earth-fixed system and the temporal derivatives of the orientation parameters are expressed by Euler's kinematical equations (Moritz and Mueller 1987).

Let $e_i^{\mathcal{H}}$ and $e_i^{\mathcal{I}}$ $(i = 1, 2, 3)$ be the orthonormal base vectors of the two above-mentioned reference systems. The orientation of the Earth-fixed system with respect to the space-fixed system can then be written as

$$e_i^{\mathcal{H}} = \underline{R}\, e_i^{\mathcal{I}} \,, \tag{3}$$

where $\underline{R}$ means a time-dependent rotation matrix which is customarily composed of four parts (Richter 1995, McCarthy and Capitaine 2002):

$$\underline{R} = \underline{W}\, \underline{S}\, \underline{N}\, \underline{P} \,. \tag{4}$$

The matrices $\underline{P}$ and $\underline{N}$ stand for precession and nutation, respectively. The matrix $\underline{S} = R_3(\theta)$ is a spin at the so-called Earth rotation angle θ around the axis of the Celestial Intermediate Pole. $\underline{W}$ accounts for the components x and y of polar motion.

The transition from the space-fixed system $\mathcal{I}$ to the Earth-fixed system $\mathcal{H}$ is depicted as follows:

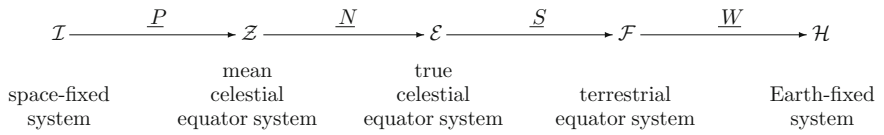

Today's fundamental astronomical space-fixed reference system is the *International Celestial Reference System* (ICRS) which was established by the International Astronomical Union (IAU) in 1997 (Feissel and Mignard 1998). The ICRS is a kinematically non-rotating coordinate system of high precision. Its origin is defined to be at the barycentre of the solar system. The ICRS which replaced the previous Fundamental Catalogue FK5 (Fricke et al. 1988) is realised in the radio frequency domain by the International Celestial Reference Frame (ICRF). The ICRF is described by equatorial coordinates of extragalactic and compact radio sources which are estimated from VLBI observations (Ma et al. 1998). At optical wavelengths the ICRS is realised by the Hipparcos catalogue. In 1998 the ICRF contained coordinates of 608 radio sources, and up to now 109 additional sources have been added by two extensions ICRF-Ext.1 and ICRF-Ext.2 (Fey et al. 2004; Gontier et al. 2006). A total of 212 very compact sources are used in order to define the axes of the reference frame (so-called defining sources). Presently the ICRF sources are observed with an accuracy of about 0.1 mas. VLBI is not capable of realising a geocentric ICRS, since it is a purely geometrical observation technique which does not provide any relation to the Earth's centre of mass. A Geocentric Celestial Reference Frame (GCRF) can be computed by combining VLBI and satellite observations or by referencing VLBI stations in a satellite-based geocentric reference frame (Seitz 2009). If the origin of the ICRS is shifted from the barycentre of the solar system into the Earth's centre of mass (under consideration of relativistic effects), the system experiences slight accelerations due to the motion of the Earth around the

Sun. Strictly speaking, such a Geocentric Celestial Reference System (GCRS) is no longer an inertial system. Commonly it is referred to as a *quasi-inertial system*.

As a consequence of its rotation the Earth is flattened at the poles. Since the Sun and Moon are generally located above or underneath the equatorial plane, a gravitational torque forces the equatorial plane towards the ecliptic (Torge 2001). Due to Earth rotation, this external force results in the precession of the Earth axis around the pole of the ecliptic, around which the rotation axis revolves on a cone with an apex angle of 23.5°. The vernal equinox that marks the intersection point of equatorial plane, ecliptic plane and the celestial sphere performs a clockwise motion at a rate of approximately 50.3″ per year along the ecliptic. In about 25,800 years, one so-called Platonic year, the vernal equinox performs one complete revolution around the celestial sphere. The precession matrix $\underline{P}$ describes the transition from the quasi-inertial GCRS into the *mean celestial equator system* $\mathcal{Z}$ (Capitaine et al. 2002; Rothacher 2002).

Precession is superposed by the lunisolar nutation, which causes variations of the Earth rotation axis in the mean celestial equator system. Lunisolar nutation is a consequence of the periodically changing positions of the Moon and Sun relative to the Earth. It is composed of various oscillations with different amplitudes and periods between few days and 18.6 years with respect to the space-fixed system (Mathews et al. 2002). The most prominent fraction of nutation is caused by the inclination of the lunar orbit by about 5° with respect to the ecliptic (Torge 2001). The orbital node, i.e. the intersection line of the lunar orbital plane and the ecliptic, moves with a period of 18.6 years along the ecliptic. As a consequence, the normal vector of the lunar orbital plane revolves along a cone around the ecliptic normal vector. The torque exerted by the Moon on the flattened Earth varies with the same period: it is maximum when the node of the lunar orbit coincides with the intersection line of equatorial plane and ecliptic and the Moon reaches its maximum declination of +28.5° or −28.5°. Further nutation terms are caused by the motion of the Moon and Sun between the northern and southern hemispheres. They feature periods of half a month and half a year, respectively (Torge 2001). With an apex angle of less than 10″, nutation is significantly smaller than precession. The nutation matrix $\underline{N}$ describes the transformation between the mean celestial equator system and the *true celestial equator system* $\mathcal{E}$.

The pole of the true celestial equator system is also known as the Celestial Intermediate Pole (CIP). According to resolution B1.7 adopted by the IAU in the year 2000 the CIP has superseded the previously used Celestial Ephemeris Pole (CEP) since 1 January 2003 (Capitaine 2002; McCarthy and Petit 2004). In pursuance of this IAU resolution, the CIP is defined as the axis with respect to which the Earth rotation angle is defined. The location of the CIP in the Earth-fixed reference system is provided by the International Earth Rotation and Reference Systems Service (IERS) on the basis of space geodetic observations and underlying models. The CIP is defined in such a way that it performs motions with periods longer than 2 days with respect to the space-fixed reference system. In the Earth-fixed system, retrograde motions of the CIP with frequencies between 0.5 and 1.5 cycles per sidereal day are allocated to nutation, whereas all other motions are interpreted as

polar motion. The change of the concept from the CEP to the CIP required the introduction of the revised model for precession and nutation IAU 2000A (Souchay et al. 1999; Mathews et al. 2002) according to resolution B1.6 of the IAU in the year 2000 (McCarthy and Petit 2004). A comprehensive overview of the IAU 2000 resolutions and their implications is given by Kaplan (2005).

If the Earth were solid and external torques were neglected, its instantaneous rotation axis would be directed towards the CIP. But in reality there is a small deflection between the CIP and the instantaneous rotation axis which is known as Oppolzer motion (Schödlbauer 2000; Capitaine 2004). As a consequence of precession and nutation, the Earth rotation axis changes its direction with respect to the space-fixed reference system as a function of time. Associated variations of right ascension and declination of fixed stars must be taken into account in astronomical observations from the Earth surface. The (true) latitude of a station, i.e. the angle between the true equatorial plane and the zenith of the station, is unaffected by precession and nutation. Matrices $\underline{P}$ and $\underline{N}$ can be modelled and predicted on the basis of lunar and solar ephemerides with high accuracy (Lieske et al. 1977; Wahr 1981; Seidelmann 1992). Small corrections to the current model (*celestial pole offsets*) are routinely published by the IERS on its internet site (http://www.iers.org). They account for model imperfections as well as for unpredictable geophysical signals such as the free core nutation or the quasi-annual oscillation of the S1 thermal tide (Dehant et al. 1999; Vondrak et al. 2005). Together with the precession–nutation model IAU 2000A, the celestial pole offsets allow for a precise computation of the location of the CIP in the space-fixed GCRF as illustrated in Fig. 6.1 (coordinates X and Y).

The transformation between $\mathcal{E}$ and the Earth-fixed system $\mathcal{H}$ is carried out on the basis of the so-called *Earth rotation parameters*. The rotation matrix $\underline{S}$ describes the diurnal rotation around the z-axis of the true celestial equator system. It is applied in order to transform between the true celestial equator system and the *terrestrial equator system* $\mathcal{F}$. Before 1 January 2003 the matrix $\underline{S}$ was related to the Greenwich Apparent Sidereal Time (GAST), i.e. the apparent hour angle of Greenwich with respect to the true vernal equinox. GAST is related to the Greenwich Mean Sidereal

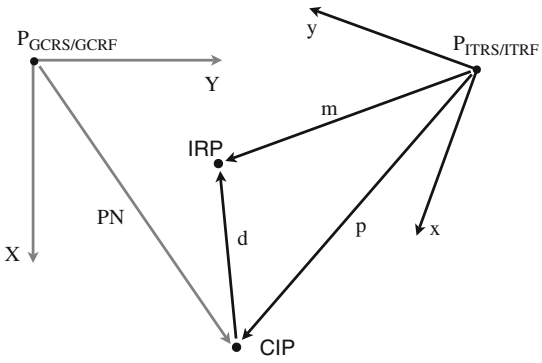

Fig. 6.1 Poles of reference with regard to the coordinate systems ITRS and GCRS (and their respective realisations ITRF/GCRF), and correspondence between model values $m(t)$ and published polar motion values $p(t)$ (Mendes Cerveira et al. 2009)

Time (GMST), i.e. the Greenwich hour angle of the mean vernal equinox, by the equation of equinoxes. From GMST universal time UT1 can be accessed (Aoki et al. 1982). According to the IAU resolution B1.8 (2000) and its supplement (IAU resolution B2, 2006), the vernal equinox as the direction of reference for the sidereal rotation of the Earth is now replaced by the so-called Celestial Intermediate Origin (CIO) in the space-fixed reference system (Capitaine 2002, 2008; McCarthy and Petit 2004). The CIO represents a non-rotating origin (Guinot 1979; Aoki and Kinoshita 1983) and is defined in such a way that the rotation vector of the celestial equator system with regard to a space-fixed reference system has no component in the direction of the CIP. The motion of the CIO relative to the space-fixed reference system has no component along the equator but a perpendicular one. Analogously a Terrestrial Intermediate Origin (TIO) is defined: the rotation vector of the terrestrial equator system with regard to an Earth-fixed reference system has no component in the direction of the CIP, and the motion of the TIO relative to the Earth-fixed reference system has solely a component perpendicular to the equator (Guinot 2002). In this concept GAST is replaced by the *Earth rotation angle* θ that is defined as the angle measured along the equator of the CIP between the unit vectors directed towards CIO and TIO. Since the direction of reference for UT1 moves uniformly along the equator, UT1 and θ are linearly related. The implementation of the IAU resolution B1.8 (2000) allows for a rigorous definition of the sidereal rotation of the Earth and for describing the rotation of the Earth independently from its orbital motion (McCarthy and Petit 2004).

The last part of the rotation matrix $\underline{R}$, the polar motion matrix $\underline{W}$, describes the transformation from the terrestrial equator system into the Earth-fixed system $\mathcal{H}$. The z-axis of the terrestrial equator system $\mathcal{F}$ is directed towards the CIP, while the z-axis of the terrestrial system is directed towards the Conventional Terrestrial Pole (CTP). Today the defined CTP is the *IERS Reference Pole*, which replaced the *Conventional International Origin* in the year 1967. The Conventional International Origin is identical with the mean direction of the Earth rotation axis between 1900 and 1905. The IERS Reference Pole differs from the Conventional International Origin by a maximum $\pm 0.03''$ and is realised by coordinates of globally distributed geodetic markers by means of space geodetic observations. Today's conventional Earth-fixed system $\mathcal{H}$ is the *International Terrestrial Reference System* (ITRS). Its origin is defined to be in the centre of mass of the Earth including atmosphere and ocean, and the z-axis of the right-hand system is directed towards the IERS Reference Pole. The orientation of the x-axis of the ITRS was originally defined by the Bureau International de l'Heure (BIH) for the epoch 1984.0. From this time, the evolution of the orientation was ensured by a no-net-rotation condition with regard to horizontal tectonic motions over the whole Earth (McCarthy and Petit 2004). The ITRS is realised by the determination of three-dimensional positions and velocities of geodetic observatories using space geodetic techniques. The most recent realisation of the ITRS is the ITRF2008. For details regarding the ITRF computation strategy see Altamimi et al. (2007).

Both the orientation of the rotation axis with respect to the CTP and the angular velocity of Earth rotation are influenced by transient, episodic and periodic exogenous and endogenous processes in the Earth system. Therefore the rotation

matrices $\underline{S}$ and $\underline{W}$ cannot be described or even predicted by models with satisfying accuracy. The IERS publishes different sets of Earth Orientation Parameters (EOP) in its circulars as well as on its internet site. Among the available parameters are the previously mentioned celestial pole offsets, the pole coordinates x_p and y_p and $\Delta\mathrm{UT} = \mathrm{UT1} - \mathrm{UTC}$. The pole coordinates x_p and y_p represent the misalignment between CIP and IERS Reference Pole, where the orientation of the x_p-axis is consistent with the x-axis of the ITRS, and the y_p-axis is directed towards 90° western longitude. The parameters x_p and y_p allow for the transformation between the terrestrial equator system $\mathcal{F}$ and the Earth-fixed system $\mathcal{H}$. Due to polar motion, the (true) latitude and longitude of a station on the Earth's surface vary with time.

Except for a constant offset due to the consideration of leap seconds, the coordinated universal time UTC corresponds to the uniform Temps Atomique International TAI which is realised by a set of worldwide distributed atomic clocks (BIPM 2007). Alternative to the parameter ΔUT, the expression *excess length-of-day* (ΔLOD) is common. ΔLOD is related to the absolute value of the Earth rotation vector in the terrestrial equator system and denotes the length of a solar day (length-of-day, LOD) expressed in UTC or TAI reduced by 86,400 s (Moritz and Mueller 1987):

$$\Delta\mathrm{LOD} = \mathrm{LOD} - 86,400\,\mathrm{s}\,. \tag{5}$$

ΔLOD and ΔUT are related according to

$$\Delta\mathrm{LOD} = -\frac{\mathrm{d}}{\mathrm{d}t}\Delta\mathrm{UT}\cdot 86,400\,\mathrm{s}\,. \tag{6}$$

Figuratively speaking, the term ΔLOD expresses the variation of the Earth's angular velocity due to geophysical and gravitational influences as a variation of the effective time for one full revolution. In former times ΔUT was observed by astronomical methods. Nowadays this parameter is unambiguously determined by VLBI due to its connection to the quasi-inertial reference frame of extragalactic radio sources. Global Navigation Satellite Systems (GNSS) allow for a precise observation of ΔLOD on short time scales.

6.2 Polar Motion

Figure 6.2 shows the Earth's polar motion between 1962 and 2009 as observed by astrometric and space geodetic observation techniques. The displayed values are taken from the well-known series EOP 05 C04 (Bizouard and Gambis 2009), in which the IERS publishes Earth orientation parameters together with respective formal errors at daily intervals since 1962. Values in this series are provided with respect to the precession–nutation model IAU 2000A and are consistent with the ITRF2005. Today polar motion can be determined with an accuracy of better than 0.1 mas (IERS 2008).

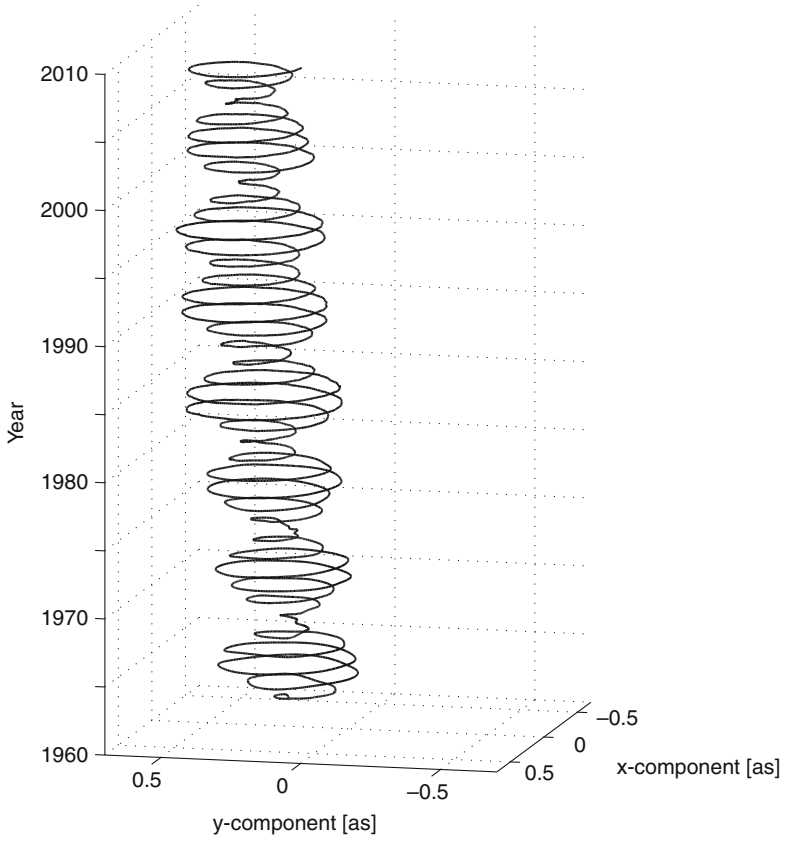

Fig. 6.2 Observations of polar motion from the EOP 05 C04 series of the IERS between 1962 and 2009

A clear beat with a period of 6.3 years is obvious. It is caused by the superposition of a signal component with annual period (approx mean amplitude 0.09″) and an oscillation with a period of about 1.2 years (approx mean amplitude 0.17″). The resulting beat amplitude is up to 0.25″ which corresponds to approximately 9 m on the Earth's surface.

While the annual oscillation can be explained by gravitational and geophysical effects within the Earth system, the oscillation with a period of 1.2 years is a free rotational mode of the Earth. It was discovered by Chandler (1891, 1892) and is therefore known as *Chandler oscillation*. The Chandler oscillation originates from a misalignment of the polar principal axis of inertia (figure axis) and the rotation axis of the Earth (Schödlbauer 2000). This causes a tumbling motion of the flattened Earth gyro, in which the rotation vector revolves on a cone around the figure axis. The Chandler oscillation is a prograde polar motion, i.e. counter-clockwise when seen from the North Pole. The existence of such a free oscillation of the Earth had

earlier been predicted by Euler (1765). From theoretical computations for a solid body with the Earth's dimension, he determined a period of 304 days (Euler period) for one revolution. Since the Earth is deformable, the actual period is lengthened to about 432 days (Chandler period) (see Sect. 6.4.2.1).

Signal decomposition of observed polar motion by means of wavelet filtering (Seitz and Schmidt 2005) allows for splitting the entire signal into its two main constituents, i.e. the Chandler oscillation and the annual oscillation. The resulting time series (x-components) are shown in Fig. 6.3 for a period of 150 years between 1860 and 2009. Since both signal components are almost circular, the y-components look very similar. Displayed values for polar motion are taken from the long-term C01 series, in which the IERS provides observations made since 1846 in a temporal resolution of 0.1 years (1846–1889) and 0.05 years (1890–2009). During the first decades the observations were based on optical astrometry and are comparatively inaccurate (standard deviations up to $\sigma = 0.16''$). The top panel of Fig. 6.3 shows the x-component of the time series C01 (after removal of a linear trend) together with the 3σ error margin. The Chandler oscillation (middle) features much stronger amplitude variations than the annual signal (bottom) which has been rather uniform during the last century (the first and the last years in the plot should not be interpreted due to boundary effects of the applied filter). Although the accuracy of the older astrometrical data is rather poor, the displayed amplitude variations are significant since the signal exceeds some 100 mas.

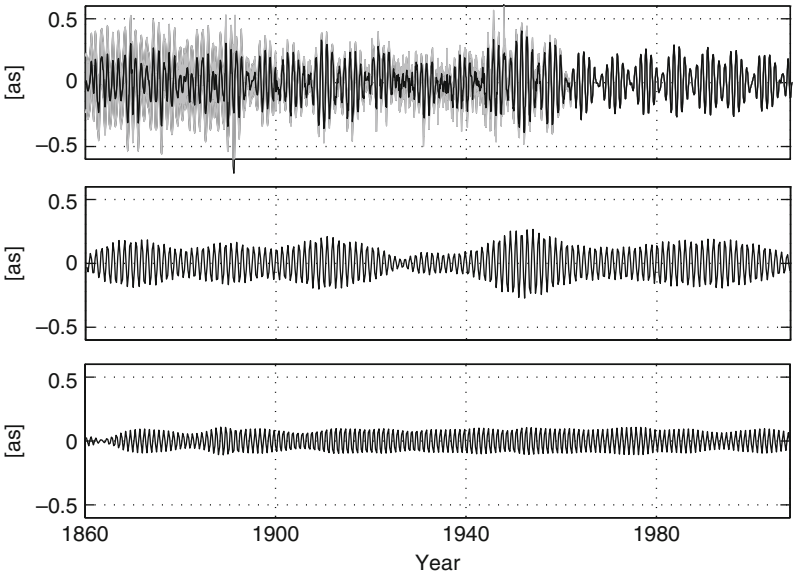

Fig. 6.3 Long-term observations of polar motion (x-component, linear trend removed) between 1860 and 2009 together with the 3σ error margin plotted in grey (*top*) and Chandler (*middle*) and annual (*bottom*) signal component determined by wavelet filtering

The origin of the strong amplitude variations and therewith the causative mechanism for the evocation of the Chandler oscillation have been under discussion for many years. As a consequence of the anelasticity of the Earth mantle and the associated dissipation due to friction, the Chandler oscillation is a damped oscillation. But the observations indicate that the amplitude of the free polar motion is excited by some mechanism which counteracts the damping. In numerous publications this matter has extensively been discussed. It has been investigated whether atmospheric or hydrologic mass redistributions (Wahr 1983; Hameed and Currie 1989; Sidorenkov 1992; Furuya et al. 1996, 1997) or processes in the Earth's interior (Souriau and Cazenave 1985; Gross 1986; Hinderer et al. 1987) are the hurriers of the oscillation. Since the Chandler oscillation is a resonance oscillation of the Earth, potential excitation mechanisms require energy in a band close to the Chandler frequency in order to excite the free polar motion and thus to counteract its damping. In recent years a number of studies came to the conclusion that the Chandler oscillation is excited by the combined effect of atmosphere and ocean (Gross 2000; Brzezinski and Nastula 2000; Seitz and Schmidt 2005). However, the individual contributions of these two subsystems could still not be fully assessed, since all investigations are naturally dependent on imperfect model assumptions of atmospheric and oceanic processes and their related mass transports. Furthermore, minor effects from continental hydrosphere, cryosphere and other subsystems must also be taken into account in order to close the budget of polar motion excitation.

The annual signal of polar motion originates similarly to a number of further significant higher and lower frequencies from gravitational and internal geophysical excitations, causing mass redistributions and mass motions within and between the Earth's subsystems. An overview of important drivers and the corresponding signatures in polar motion (amplitudes and periods) is given by Chao (1994) and Gross (2007). As mentioned above, there are also singular and non-periodic contributions from transient and episodic geophysical effects, such as earthquakes (Chao and Gross 1987, 2005) or El Niño situations (Kosek et al. 2001). Forced variations of polar motion and the free Chandler oscillation are closely linked. Variations of the Earth rotation vector induce a change of the Earth's centrifugal potential which leads to additional mass redistributions in the solid Earth and the ocean (so-called rotational deformations). This back-coupling effect causes a motion of the principal axis of inertia that affects the Chandler oscillation (see Sect. 6.4.2.1).

Figure 6.4 shows the polar motion curve in units of metres on the Earth surface in more detail for a time interval of 6 months (Schreiber et al. 2004). The large circle results from the superposition of signal components with comparatively long periods (especially the prograde Chandler and pro- and retrograde annual oscillations), whereas the small circles with magnitudes of approximately $0.01''$ are nearly diurnal retrograde polar motion components which are related to corresponding precession and dominant nutation terms in the space-fixed reference system (Oppolzer terms). The pronounced beat effect with a period of 13.7 days results from the superposition of oscillations that correspond to precession (period 0.997 days in the Earth-fixed reference system) and the largest nutation term (period 1.076 days in the Earth-fixed reference system). Variations of the beat amplitude are caused by further signal components that correspond to other nutation terms with approximately diurnal period

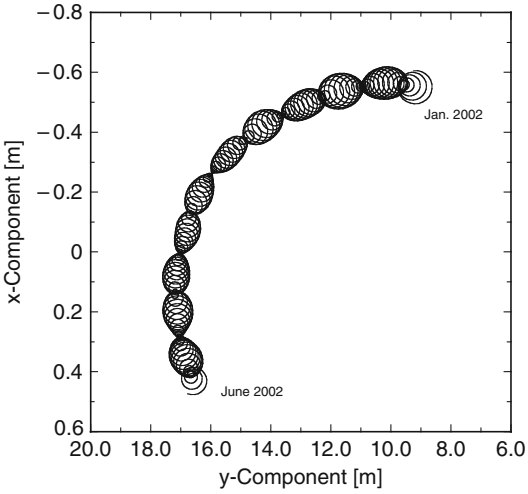

Fig. 6.4 Path of the rotation pole in the Earth-fixed reference system between January and June 2002 in metres on the Earth surface (Figure taken from Schreiber et al. 2004)

in the Earth-fixed system (McClure 1973). In analogy to precession and nutation in the space-fixed system, the retrograde nearly diurnal polar motion in the terrestrial system originates from lunisolar gravitational torques on the equatorial bulge of the Earth. Earth rotation causes a daily variation of the gravitational forces which results in the almost circular motion of the rotation pole in the direction opposite to the rotation. Nearly diurnal retrograde polar motion cannot be directly assessed by observations of VLBI, SLR/LLR and GNSS since these techniques are sensitive only to the complete rotation matrix from the Earth-fixed to the space-fixed reference frame from which no discrimination between celestial pole offsets and nearly diurnal retrograde polar motion is possible. An inertial rotation sensor on the Earth's surface is sensitive to the diurnal retrograde polar motion since the angle between the axis of the instrument and the rotation axis of the Earth changes with a period of 1 day. In this way, ring laser gyroscopes allow for the direct observation of the position of the instantaneous rotation axis and therewith for the assessment of the diurnal polar motion (Schreiber et al. 2004).

Beside the periodic and irregular fluctuations, polar motion is characterised by a secular trend at a present rate of 3.3 mas/a in the direction of 76°–78° western longitude (Vondrak et al. 1995; Schuh et al. 2001). Although the reason is not entirely understood yet, there is evidence that this secular motion is caused by postglacial rebound and sea-level variations (Milne and Mitrovica 1998).

6.3 Variations of Length-of-Day and ΔUT

The variation of the length of a solar day (ΔLOD) can be determined from the observations of modern space geodetic techniques with an accuracy of 20μs (IERS 2008). As shown in (6) ΔLOD is directly related to ΔUT. While accurate short-term time series of ΔLOD, i.e. of the derivative of ΔUT, can be estimated with high temporal resolution from GNSS observations, mid-term and long-term stability

of ΔLOD as well as ΔUT series can only be guaranteed by VLBI, providing the connection to the quasi-inertial reference frame. All satellite-based techniques, such as GPS or Glonass, meet the problem that Earth rotation cannot be distinguished from a uniform rotation of the satellite orbit nodes (Ray 1996).

Figure 6.5 (top panel) displays the observed variations of length-of-day from the EOP 05 C04 of the IERS for the period between 1962 and 2009. The curve is dominated by a secular signal of the order of milliseconds that is superposed by significant variations with annual and semi-annual periods due to mainly atmospheric effects and tidal signals with periods of several days. In contrast to polar motion, there is no free variation of length-of-day due to rotational deformations (Wahr 1985). The decadal variability of ΔLOD is ascribed to the exchange of angular momentum between the Earth's core and mantle (Liao and Greiner-Mai 1999). This assumption is supported by strong correlations between the decadal variations of ΔLOD with fluctuations of the Earth's magnetic field (Schuh et al. 2003). Four potential mechanisms of core–mantle coupling (CMC) are presently under discussion: topographic, electromagnetic, viscoelastic and gravitational coupling. Available models of topographic coupling are rather inaccurate since the knowledge of the topography at the core–mantle boundary is insufficient. But presumably this coupling mechanism does not provide enough energy in order to excite the strong variations of ΔLOD (Ponsar et al. 2002). Holme (1998) showed that the electromagnetic CMC seems to be the most important excitation mechanism. It is based on variations of the geomagnetic field due to dynamo processes, which exert a torque on conductive regions of the lower mantle via the Lorentz force (Schuh et al. 2003). Viscoelastic and gravitational coupling are inferior. In the frame of its *Special Bureau for the Core* (SBC) of the Global Geophysical Fluids Center (GGFC), the IERS provides model time series that describe the effects of CMC on ΔLOD. In Fig. 6.5b the results of three different models are compared with a moving average of the observations over 5 years. One of the model data sets (according to Jackson, Bloxham and Gubbins, JBG) has a temporal resolution of 1 year (Jackson 1997); the other two models (according to Petrov and Dehant, PD1 and PD2) are available for intervals of 5 years. All data sets are based on the frozen flux hypothesis (Jault et al. 1988). While JBG is a free model, PD1 and PD2 are based on observations of the magnetic field. The comparison of the various models provided by the SBC reveals significant differences. To a certain extent the data series correspond with the moving average (especially in the case of PD2), but the temporal resolution is much too coarse to explain the decadal variations of ΔLOD with sufficient accuracy and thus to exclude other causative processes.

Variations of ΔLOD on annual, seasonal and shorter time scales are highly correlated with angular momentum fluctuations within the atmosphere (mainly due to zonal winds) and, to a minor extent, due to ocean currents. The two strongest signal components induced by those processes, i.e. the annual and semi-annual oscillation, feature almost equal amplitudes of approximately 0.36 ms. In addition, there is a weak quasi-biennial oscillation (QBO) due to irregular variations of zonal winds and temperatures in the tropical troposphere and stratosphere (Trenberth 1980). Its amplitude varies from cycle to cycle. In general it is smaller than 0.1 ms (Höpfner

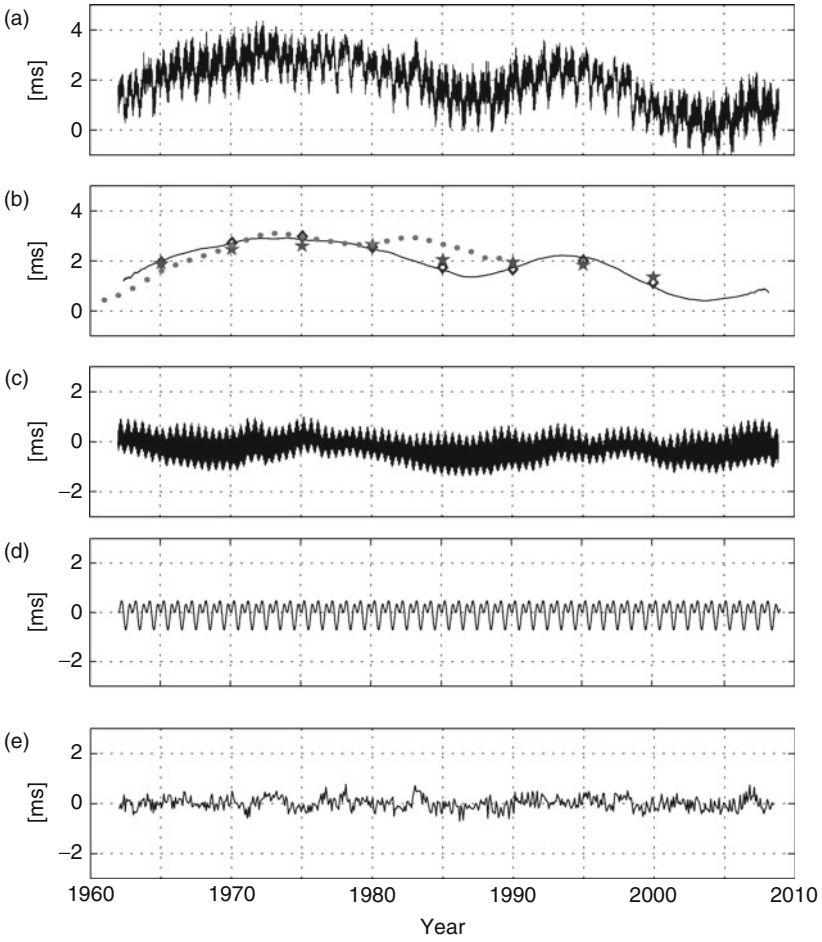

Fig. 6.5 Variations of length-of-day (ΔLOD) for the time frame between 1962 and 2009. (**a**) Observation time series EOP 05 C04. (**b**) Moving average over 5 years in comparison with three models for the influence of core–mantle interaction (dots: JBG; stars: PD1; diamonds: PD2; see text). (**c**) Effect of solid Earth tides. (**d**) Annual and semi-annual signal component. (**e**) Residual time series (**a-b-c-d**)

2001). The most important periods induced by solid Earth tides are 9.13 days (amplitude 0.07 ms), 13.63 days (0.15 ms), 13.66 days (0.35 ms) and 27.55 days (0.19 ms) (Yoder et al. 1981; McCarthy and Petit 2004). In contrast to solid Earth tides, the influence of ocean tides on ΔLOD is small (Lambeck 1980; Gross 1993), but not negligible in high-precision space geodesy.

The residual signal of ΔLOD (Fig. 6.5e), i.e. after reduction of the decadal signal, the annual and semi-annual oscillations and the tidal effects feature transient increases of the length-of-day during 1983 and (somewhat less pronounced) during 1997. These episodic signals can be explained by strong El Niño events (Rosen et al.

1984; Chao 1989). Like polar motion, ΔLOD is characterised by a secular change. Especially as a consequence of tidal friction, the length of a solar day increases by 2.3 ms per century (Morrison and Stephenson 1998).

6.4 Physical Model of Earth Rotation

6.4.1 Balance of Angular Momentum in the Earth System

From a physical perspective, Earth rotation can be interpreted as the rotary motion of a multitude of individual and interrelated mass elements about one common axis. This rotary motion is comparable to that of a physical gyroscope. Therefore theoretical and numerical studies on temporal variations of Earth rotation are based on equations of gyroscopic motion which follow from the balance of angular momentum in the Earth system. With respect to an Earth-fixed, i.e. rotating, reference system, the balance between the Earth's angular momentum $\mathbf{H}$ and external torques $\mathbf{L}$ due to, e.g., lunisolar and planetary gravitational forces is described by the dynamic Euler equation (Lambeck 1980):

$$\frac{\mathrm{d}}{\mathrm{d}t}\mathbf{H} + \boldsymbol{\omega} \times \mathbf{H} = \mathbf{L} \,. \tag{7}$$

In this equation $\boldsymbol{\omega}$ denotes the rotation vector of the Earth with respect to the rotating reference system. The angular momentum of a rotating rigid body equals the product of its tensor of inertia $\underline{\mathbf{I}}$ and the rotation vector $\boldsymbol{\omega}$:

$$\mathbf{H} = \underline{\mathbf{I}} \cdot \boldsymbol{\omega} \,. \tag{8}$$

The symmetric tensor of inertia describes the mass distribution in the system (Lambeck 1980). In the case of a rigid body it is invariant with respect to body-fixed axes:

$$\underline{\mathbf{I}} = \int\int\int \rho(x,y,z) \begin{pmatrix} y^2+z^2 & -xy & -xz \\ -xy & x^2+z^2 & -yz \\ -xz & -yz & x^2+y^2 \end{pmatrix} \mathrm{dV} \,, \tag{9}$$

where $\rho(x, y, z)$ is the density at the three-dimensional position (x, y, z). In the case of a rotating deformable body, the angular momentum $\mathbf{H}$ is split into two parts: one fraction corresponds to the angular momentum of the rotating rigid body (8), but with the difference that the tensor of inertia is now time variable due to deformability. The second fraction can be viewed as angular momentum $\mathbf{h}$ relative to the body rotation. It follows from the motion of mass elements with velocity $\mathbf{v}^{\mathrm{rel}}$ relative to the rotating reference system, in which the rotation is described:

$$\mathbf{h} = \int\int\int \rho(x,y,z) \cdot (\mathbf{r} \times \mathbf{v}^{\mathrm{rel}})\, d\mathrm{V} \,, \tag{10}$$

where $\mathbf{r}$ denotes a three-dimensional position vector. Consequently the angular momentum of a rotating deformable body is (Schneider 1988)

$$\mathbf{H} = \underline{\mathbf{I}} \cdot \boldsymbol{\omega} + \mathbf{h} \,, \tag{11}$$

where the first summand is also referred to as *mass term*, the second one as *motion term*. Insertion of (11) into (7) yields

$$\frac{\mathrm{d}}{\mathrm{d}t}(\underline{\mathbf{I}} \cdot \boldsymbol{\omega} + \mathbf{h}) + \boldsymbol{\omega} \times (\underline{\mathbf{I}} \cdot \boldsymbol{\omega} + \mathbf{h}) = \mathbf{L} \,. \tag{12}$$

In this form the equation is also known as *Euler–Liouville* or in short *Liouville equation* (Munk and MacDonald 1960). In the context of Earth rotation studies, the term deformability not only refers to deformations of the Earth's body but also to mass redistributions within and between the various components of the Earth system. In particular, atmospheric and oceanic transport processes and related mass changes are very important on time scales from hours and days to several years. While the time-variable mass distribution in the system influences the tensor of inertia $\underline{\mathbf{I}}$, motions of mass elements with respect to the reference system cause relative angular momenta $\mathbf{h}$. Consequently all elements of the Liouville equation are time variable:

$$\underline{\mathbf{I}} = \underline{\mathbf{I}}(t), \ \mathbf{h} = \mathbf{h}(t), \ \boldsymbol{\omega} = \boldsymbol{\omega}(t), \ \mathbf{L} = \mathbf{L}(t) \,. \tag{13}$$

Angular momentum is exchanged among the individual components of the Earth system via mass transfer processes and torques. The occurrence of relative angular momenta is not necessarily linked to the appearance of variations of the tensor of inertia. Certainly most of the relevant processes influence both the mass and the motion term simultaneously. For instance, the atmospheric flow is generally related to variations of atmospheric pressure, and ocean circulation is usually accompanied by variations of ocean bottom pressure. But on the other hand mass motions are conceivable that do not influence the mass distribution in the Earth system and consequently the tensor of inertia. This is the case if one mass element is instantaneously replaced by a subsequent one (e.g. in a ring-like ocean current) or if the Earth's core experiences an acceleration with respect to the Earth's mantle. Vice versa vertical deformations of the Earth as a consequence of loading or the time-variable snow coverage could be mentioned as examples of mass redistributions without a significant influence on the motion term.

In theoretical studies on Earth rotation, the quantities in the Liouville equation are often related to a rotating reference system, according to which the mass elements of a rotating rigid body are invariant with respect to their position at all times. For a deformable Earth such a system can be defined by a minimum condition (Schneider 1988). An example is the Tisserand system (Tisserand 1891), for which the integral effect of the relative motions of mass elements with respect to the reference system is minimised ($\mathbf{h} = 0$). The application of the Tisserand system simplifies the Liouville equation (12) considerably. But on the other hand the definition of the

Tisserand system is hypothetical, since relative angular momenta (especially in the Earth's interior) are not accessible from observations on the Earth's surface (Engels and Grafarend 1999).

Numerical investigations are commonly performed in a geocentric terrestrial reference system. Its rotation axis is oriented towards the polar moment of inertia C of the Earth, its x-axis is directed towards the Greenwich meridian and its y-axis towards 90°E. The terrestrial system performs a uniform rotation about its z-axis with angular velocity $\Omega = 2\pi/86,164\,\mathrm{s}$. Temporal variations of the instantaneous Earth rotation vector $\boldsymbol{\omega}(t)$ are viewed as small deviations of the uniform rotation. In coordinates of the terrestrial system the Earth rotation vector is expressed as (Munk and MacDonald 1960)

$$\boldsymbol{\omega}(t) = \Omega \cdot \begin{pmatrix} m_1(t) \\ m_2(t) \\ 1 + m_3(t) \end{pmatrix}, \qquad m_i \ll 1 \,. \tag{14}$$

The dimensionless quantities $m_i(t)\,(i = 1, 2, 3)$ represent slight disturbances of the uniform rotation (Munk and MacDonald 1960). The two components $m_1(t)$ and $m_2(t)$ describe the time-variable orientation of the rotation axis with respect to the z-axis of the terrestrial system (polar motion). Deviations of the Earth's angular velocity with respect to Ω are associated with changes of the length-of-day. They follow from the temporal variation of the absolute value of the Earth rotation vector $|\boldsymbol{\omega}(t)|$ (Lambeck 1980; Schneider 1988):

$$|\boldsymbol{\omega}(t)| = \Omega \sqrt{m_1(t)^2 \; + m_2(t)^2 \; + (1 + m_3(t))^2} \quad \approx \quad \Omega\,(1 + m_3(t)) \,. \tag{15}$$

The error of ΔLOD due to this approximation is 10^{-16} s and therefore negligible.

The Earth's tensor of inertia $\underline{\mathbf{I}}(t)$ can be interpreted as the sum of two components $\underline{\mathbf{I}}_0$ and $\Delta\underline{\mathbf{I}}(t)$ (Lambeck 1980), where $\underline{\mathbf{I}}_0$ is an approximate tensor. If the axes of the reference system coincide with the principal axes of inertia, the approximate tensor has a diagonal structure:

$$\underline{\mathbf{I}}_0 = \begin{pmatrix} A & 0 & 0 \\ 0 & B & 0 \\ 0 & 0 & C \end{pmatrix} \,, \tag{16}$$

where A and B are the equatorial principal moments of inertia and C is the axial principal moment of inertia of the Earth ($C > B > A$). But the axes of the principal moments of inertia differ from the axes of the previously described terrestrial reference system by approximately 15° in the equatorial plane (Marchenko and Schwintzer 2003). This divergence has to be taken into account by means of a rotation. Consequently $\underline{\mathbf{I}}_0$ does not have a diagonal structure with respect to the axes of the applied terrestrial system.

Due to mass redistributions in the Earth system, small time-dependent deviations $\Delta\underline{\mathbf{I}}(t)$ of the approximate tensor $\underline{\mathbf{I}}_0$ arise (Moritz and Mueller 1987). With the

tensor elements (so-called deviation moments) $c_{ij}(t) \ll A, B, C\,(i,j = 1,2,3)$ the symmetric tensor $\Delta\underline{\mathbf{I}}(t)$ reads

$$\Delta\underline{\mathbf{I}}(t) = \begin{pmatrix} c_{11}(t) & c_{12}(t) & c_{13}(t) \\ & c_{22}(t) & c_{23}(t) \\ \text{sym.} & & c_{33}(t) \end{pmatrix} . \tag{17}$$

If deviations of the tensor $c_{ij}(t)$, relative angular momenta $\mathbf{h}(t)$ and external torques $\mathbf{L}(t)$ are provided from models or observations, the solution of the Liouville Equation for $\boldsymbol{\omega}(t)$ allows for the forward computation of Earth rotation variations. The relation between modelled values $m_i(t)$ and geodetic observations will be discussed in Sect. 6.5.

Two different approaches, the angular momentum approach and the torque approach, are in principle applicable for the set-up and solution of the Liouville equation. Theoretically both approaches are equivalent, but they differ conceptually with respect to their view of the Earth system. Accordingly, the procedures of modelling effects of the Earth's fluid components (e.g. atmosphere, ocean, continental hydrosphere) on Earth rotation are different (De Viron et al. 2005).

6.4.1.1 Angular Momentum Approach

The angular momentum approach is the classical approach for modelling Earth rotation. It has been described in various publications (Munk and MacDonald 1960; Lambeck 1980; Barnes et al. 1983; Moritz and Mueller 1987). The rotating body for which the Liouville equation is set up comprehends the solid Earth, atmosphere, hydrosphere and all other subsystems. In the absence of external lunisolar and (much smaller) planetary torques, this system of mass elements is viewed to be isolated, i.e. the right-hand side of (12) is zero, and the total angular momentum of the rotating body is conserved. Fractions of angular momentum can be transferred between the individual system components by redistributions and motions of masses. Changes of the angular momentum due to atmospheric, oceanic and other dynamic processes are associated with an opposite change of angular momentum of the solid Earth which is accompanied by variations of the Earth rotation vector $\boldsymbol{\omega}(t)$.

In the angular momentum approach, solely gravitational torques from external celestial bodies act on the rotating Earth. If the Sun, Moon and planets are viewed as point masses, the gravitational torque $\mathbf{L}(t)$ on the right-hand side of the Liouville equation (12) can be written as (Moritz and Mueller 1987; Beutler 2005)

$$\mathbf{L}(t) = \sum_j \frac{3GM_j}{r_{ej}^5(t)} \begin{pmatrix} y_j(t)\, z_j(t)\, (C-B) \\ x_j(t)\, z_j(t)\, (A-C) \\ x_j(t)\, y_j(t)\, (B-A) \end{pmatrix} . \tag{18}$$

In this equation G is the gravitational constant, and index j stands for the respective celestial body with the (point-)mass M_j; its geocentric distance is denoted with $r_{ej}(t); x_j(t), y_j(t), z_j(t)$ are its coordinates in the rotating reference system. In

its conventions the IERS recommends the use of the solar, lunar and planetary *JPL Development Ephemeris* DE405/LE405 (Standish 1998; McCarthy and Petit 2004).

Each relocation of mass elements within the system leads to an instantaneous change of the tensor of inertia $\Delta\underline{\mathbf{I}}(t)$. Deviation moments $c_{ij}(t)$ for the solid Earth result from deformations of the Earth's body as reaction to a tide generating potential, rotational variations and surface mass loads (Moritz and Mueller 1987; Seitz et al. 2004) (see Sect. 6.4.2). Relative angular momenta $\mathbf{h}(t)$ are due to the motion of individual mass elements relative to the terrestrial reference system.

The angular momentum approach corresponds to an abstract balance of angular momentum of all subsystems. Their individual contributions to the angular momentum budget are linearly superposed:

$$\begin{aligned} \underline{\mathbf{I}}(t) &= \underline{\mathbf{I}}_0 + \Delta\underline{\mathbf{I}}_{\text{ solid Earth}}(t) + \Delta\underline{\mathbf{I}}_{\text{ atmosphere}}(t) + \Delta\underline{\mathbf{I}}_{\text{ ocean}}(t) + \cdots, \\ \mathbf{h}(t) &= \mathbf{h}_{\text{ solid Earth}}(t) + \mathbf{h}_{\text{ atmosphere}}(t) + \mathbf{h}_{\text{ ocean}}(t) + \cdots . \end{aligned} \tag{19}$$

Variations of the tensor of inertia can be computed from modelled or observation-based mass balances of the Earth's subsystems. Relative angular momenta are derived from fluxes from global atmosphere and ocean circulation models.

6.4.1.2 Torque Approach

In the torque approach the effects of the Earth's fluid components, atmosphere and ocean, on the balance of angular momentum are modelled as (quasi-)external torques (Wahr 1982). That is, the integral effect of direct atmospheric and oceanic forces on the solid Earth appears in the vector $\mathbf{L}(t)$ on the right-hand side of the Liouville equation (12). Similar to the angular momentum approach, variations of the tensor of inertia $\Delta\underline{\mathbf{I}}(t)$ are due to deformations of the solid Earth caused by tides, surface mass loads and rotational variations. Since atmosphere and ocean are viewed as external systems, their mass redistributions do not affect the tensor of inertia. Likewise there are no relative angular momenta $\mathbf{h}(t)$ due to atmospheric and oceanic currents.

Torques between atmosphere/ocean and the solid Earth are assessed on the basis of global atmosphere and ocean circulation models. The acting torque is composed of three parts: pressure torque, gravitational torque and friction torque (De Viron et al. 2001). The pressure torque acts on the Earth's topography. It is derived from fields of surface and ocean bottom pressure and the gradient of the topography. The gravitational torque is a result of the interaction between the mass distributions within atmosphere/ocean and the solid Earth. The friction torque results from the relative motion of atmosphere and ocean currents with respect to the Earth surface. Since the friction drag of the Earth's surface is widely unknown it is particularly difficult to model (De Viron and Dehant 2003a). In a study on the influence of the atmospheric torque on polar motion De Viron et al. (1999) demonstrated that the time derivatives of the equatorial atmospheric angular momentum and the sum of the atmospheric equatorial torques agree well in the spectral range of longer than 1 day. Furthermore this study revealed that the magnitude of the equatorial components of

pressure and gravitational torque are almost equal (but with opposite signs) and that both contribute significantly stronger to polar motion than the friction torque.

The effects of atmospheric and oceanic pressure torque, gravitational torque and friction torque are superposed to the previously described external gravitational torque exerted by Sun, Moon and planets (18). Therefore the total torque $\mathbf{L}(t)$ can be written as

$$\mathbf{L}(t) = \mathbf{L}_{\text{pressure}}(t) + \mathbf{L}_{\text{gravitation}}(t) + \mathbf{L}_{\text{friction}}(t) + \mathbf{L}_{\text{external}}(t) \; . \tag{20}$$

Since lunisolar and planetary torques have a discrete spectrum in narrow vicinity of the diurnal retrograde frequency, they can be modelled quite well via harmonic expansion. Atmospheric and non-tidal oceanic torques, however, have a continuous spectrum and are thus unpredictable. Consequently, the modelling has to be performed in the time domain.

From the viewpoint of physical understanding, the torque approach is superior to the angular momentum approach. By modelling explicit interactions between atmosphere/ocean and the solid Earth via particular forces, it is possible to tell which specific processes lead to a change of the angular momentum budget and thus cause variations of Earth rotation. The torque approach is ideal for geographical studies since it allows for a direct identification of regions in which the interaction between atmosphere, ocean and the solid Earth is stronger than in others (De Viron and Dehant 2003b). In this way, the approach provides valuable physical insights into dynamic interactions in the Earth system.

The largest limitation for the torque approach is the lack of sufficiently accurate numerical models for the computation of the torques due to atmospheric and oceanic pressure, gravitation and friction. While model errors are not so crucial in the case of the angular momentum approach (where the errors smooth out due to the computation of one global value), the torque approach is highly sensitive to errors (De Viron and Dehant 2003b). As stated above, many of the parameters which are necessary for the computation of torques are not well known, e.g. the friction drag between air and Earth surface or between water and ocean bottom. Furthermore, the computation of the pressure torque is unsatisfactory due to the comparatively coarse spatial resolution of available orography models (De Viron et al. 1999; Stuck 2002).

Due to these data problems, atmospheric and oceanic angular momentum values presently appear to be more reliable for the interpretation of geodetic observations of Earth rotation. Nevertheless the torque approach is promising in the light of future model advancements.

6.4.2 Solid Earth Deformations

Mass redistributions and corresponding variations of the tensor of inertia are also caused by deformations of the solid Earth as a consequence of its reaction to the lunisolar and planetary tide generating potential, variations of the centrifugal potential due to polar motion and mass loads on the Earth surface.

Theoretical considerations on the effects of solid Earth and ocean tides on Earth rotation are provided together with elaborate instructions for numerical computations in the conventions of the IERS (McCarthy and Petit 2004). For particulars the reader is referred to this publication and the references therein. The following section will focus on the deformations induced by rotational variations and surface mass loads.

6.4.2.1 Rotational Deformations

Temporal variations of the rotation vector $\boldsymbol{\omega}(t)$ lead to variations of the Earth's centrifugal potential. This causes deformations of the solid Earth and the ocean which are also known as *rotational deformations*. While vertical deformations due to variations of the angular velocity of the rotation are below 0.5 mm at the Earth surface (Wahr 1985) and therefore negligible, the effects due to polar motion are up to 25 mm (Gipson and Ma 1998). These changes of the Earth's geometry are accompanied by variations of the tensor of inertia that are superposed to other deviations $c_{ij}(t)$ $(i,j = 1,2,3)$ due to mass redistributions induced by gravity and other geophysical effects. The back coupling from polar motion to the tensor of inertia influences the Earth's rotational dynamics significantly: it is well known that rotational deformations are responsible for the prolongation of the Euler period of 304 days (which is the period of the free oscillation of a rigid body with the Earth's dimensions) to the observed period of the free oscillation of about 432 days (Chandler period) (Moritz and Mueller 1987).

The effect of polar motion on the Earth's centrifugal potential is referred to as *pole tide*. Parameters $m_1(t)$ and $m_2(t)$ of the Earth rotation vector are related to temporal variations of the coefficients $\Delta C_{21}(t)$ and $\Delta S_{21}(t)$ of the spherical harmonic expansion of the geopotential (McCarthy and Petit 2004):

$$\begin{aligned} \Delta C_{21}(t) &= -\frac{\Omega^2 a^3}{3GM_\mathrm{E}} \left(\Re(k_2) \cdot m_1(t) + \Im(k_2) \cdot m_2(t) \right) , \\ \Delta S_{21}(t) &= -\frac{\Omega^2 a^3}{3GM_\mathrm{E}} \left(\Re(k_2) \cdot m_2(t) - \Im(k_2) \cdot m_1(t) \right) , \end{aligned} \tag{21}$$

where a and M_E stand for mean equatorial radius and total mass of the Earth. The effect of polar motion on rotational deformations and therewith on the variation of the geopotential depends on the Earth's rheological properties. In (21) the rheology is described by the complex pole tide Love number $k_2 = \Re(k_2) + i\Im(k_2)$, where $\Re$ and $\Im$ stand for real part and imaginary part, respectively.

The coefficients $\Delta C_{21}(t)$ and $\Delta S_{21}(t)$ are directly linked to the elements of $c_{13}(t$ and $c_{23}(t)$ of the tensor of inertia (Lambeck 1980):

$$\begin{aligned} \Delta C_{21}(t) &= \frac{-c_{13}(t)}{a^2 M_\mathrm{E}} , \\ \Delta S_{21}(t) &= \frac{-c_{23}(t)}{a^2 M_\mathrm{E}} . \end{aligned} \tag{22}$$

If the Earth was a rigid body, i.e. if the tensor of inertia was invariant with respect to time and there were no relative angular momenta, the Earth would rotate freely at the Euler period of 304 days as stated above. In an extensive study Smith and Dahlen (1981) discussed the consequences of deformability for the period of the free polar motion and derived an appropriate numerical value of the pole tide Love number k_2 in the light of mantle anelasticity and the dynamics of core and ocean. In a first step Smith and Dahlen (1981) approximated the Earth as a purely elastic body and neglected the dynamic response of core and ocean. The pole tide Love number was introduced with the (preliminary) numerical value of $k_2^* = 0.30088$, which was computed from the hydrostatic ellipsoidal Earth model 1066A (Gilbert and Dziewonski 1975). It was shown that the period of the free rotation of a fully elastic Earth would amount to 447 days, i.e. 143 days longer than that of a rigid body.

In order to refine the Earth's reaction on rotational variations, the effects of the dynamic fluid core, the equilibrium ocean pole tides and the mantle anelasticity must be taken into account for the computation of rotational deformations. In the following a simple Earth model will be discussed which consists of an anelastic mantle and a spherical liquid core. Both are assumed to be completely decoupled. Basic considerations on the application of such a model body for studies on Earth rotation can be found in, e.g. Moritz and Mueller (1987) and Brzezinski (2001). It is similar to the models introduced by Molodensky (1961) and Sasao et al. (1980), but in contrast to the latter studies, the approach does not account for the exchange of angular momentum between core and mantle. While the effects of core–mantle coupling on polar motion are significant mainly on subdaily time scales, there are huge decadal variations of ΔLOD due to the interaction of core and mantle (see Sect. 6.3). As a consequence of the decoupling, the principal moments of inertia A, B and C which are the parameters of the approximate tensor of inertia $\underline{\mathbf{I}}_0$ (16) of the entire Earth have to be replaced by A_m, B_m and C_m, which are attributed to the mantle alone. Since the core is assumed to be spherical, the principal moments of inertia used for the computation are derived from $A_\mathrm{m} = A - A_\mathrm{c}, B_\mathrm{m} = B - A_\mathrm{c}$, and $C_\mathrm{m} = C - A_\mathrm{c}$, where A_c denotes the principal moment of inertia of the spherical core. Its value is derived from (Sasao et al. 1980)

$$A_\mathrm{c} = A\frac{\xi}{\gamma}, \tag{23}$$

where ξ and γ are constants accounting for the rheology of mantle and core. The values provided by Sasao et al. (1980) are $\xi = 2.300 \times 10^{-4}$ and $\gamma = 1.970 \times 10^{-3}$. In a later study, Mathews et al. (1991) computed $\xi = 2.222 \times 10^{-4}$ and $\gamma = 1.965 \times 10^{-3}$ from the Preliminary Reference Earth Model PREM (Dziewonski and Anderson 1981). The non-participation of the core in the rotation shortens the period of the free polar motion by approximately 50.5 days (Smith and Dahlen 1981). That is, the period of the free rotation of a fully elastic Earth with liquid core would be around 396 days.

In order to account for the effects of ocean pole tides and mantle anelasticity, surcharges to the above given value for the elastic pole tide Love number k_2^* are

added (Smith and Dahlen 1981). The effective pole tide Love number k_2 becomes

$$k_2 = k_2^* + \Delta k_2^{\mathrm{O}} + \Delta k_2^{\mathrm{A}}\,, \tag{24}$$

where Δk_2^{O} and Δk_2^{A} denote the incremental corrections of the elastic pole tide Love number due to ocean pole tides and the anelastic response of the Earth's mantle. Following Smith and Dahlen (1981) and a more recent study by Mathews et al. (2002) the appropriate addend for the contribution of equilibrium ocean pole tides amounts to $\Delta k_2^{\mathrm{O}} = 0.044$. Thereby the period of the free oscillation is lengthened by about 29.8 days (Smith and Dahlen 1981).

The reaction of the Earth's mantle on variations of the centrifugal potential is not ideally elastic. Due to friction, rotational deformations of the mantle are a dissipative process which is equivalent to an attenuation of the free polar motion. That means, in the absence of a counteracting excitation mechanism, the rotation axis of the Earth would dislocate towards its figure axis within a few decades (Moritz and Mueller 1987). The effect of mantle anelasticity causes an extension of the period of the free rotation by another 8.5 days (Wilson and Haubrich 1976). It is considered by the complex surcharge $\Delta k_2^{\mathrm{A}} = 0.0125 + 0.0036i$ to the Love number k_2^* (Mathews et al. 2002; McCarthy and Petit 2004).

Summing up the effects of ocean, core and mantle, the value of the pole tide Love number is $k_2 = 0.35 + 0.0036i$ (McCarthy and Petit 2004). This value is appropriate for a deformable Earth with a spherical liquid core, taking into account the effects of ocean pole tides and mantle anelasticity. When k_2 was applied in a numerical simulation with a dynamic Earth system model, the resulting Chandler period was 431.9 days (Seitz et al. 2004) which coincides with geodetic observations. The result of the simulation for the x-component of polar motion over a period of 100 years is displayed in Fig. 6.6 Since neither gravitational effects nor mass redistributions and motions in the Earth's fluid components have been considered in this experiment, the curve reflects the free polar motion under the influence of mantle anelasticity or – mathematically speaking – under the influence of the imaginary part of the pole tide Love number $\Im(k_2)$. The curve is provided in normalised representation since the choice of the initial values is arbitrary. The damping of the Chandler amplitude is obvious, and after already 22 years the amplitude is reduced by half.

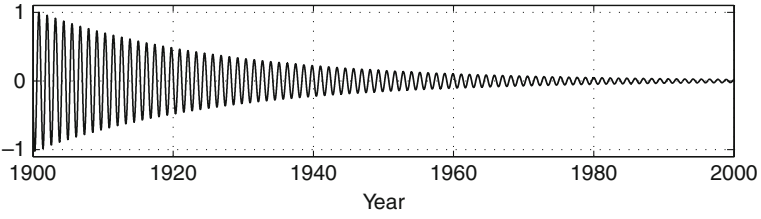

Fig. 6.6 Damped Chandler oscillation (x-component) derived from a simulation study with a dynamic Earth system model over 100 years regarding ocean pole tides and mantle anelasticity (Seitz et al. 2004)

The damping function $c(t)$ is the envelope of the oscillation

$$c(t) = c_0 \cdot e^{-\delta(t-t_0)}, \tag{25}$$

where c_0 is the initial amplitude of the oscillation and δ is the damping coefficient. The damping coefficient is derived from the proportion of two subsequent maxima of the oscillation $c_i(t_i)$ and $c_{i+1}(t_{i+1})$:

$$\delta = \frac{\ln\left(c_i/c_{i+1}\right)}{(t_{i+1} - t_i)}. \tag{26}$$

Usually the damping of the Chandler oscillation is expressed in terms of a quality factor Q. The reciprocal value Q^{-1} represents the specific dissipation, i.e. the loss of energy at the Chandler frequency (Munk and MacDonald 1960). The specific dissipation is related to the damping coefficient:

$$Q^{-1} = \frac{\delta\,(t_{i+1} - t_i)}{\pi}. \tag{27}$$

The numerical value of the quality factor that corresponds to the curve displayed in Fig. 6.6 ($k_2 = 0.35 + 0.0036i$) is $Q = 82$. In Table 6.1 values of period and quality factor of the Chandler oscillation from various studies are provided. They were computed from geodetic observations and models using different methods. Especially the quality factor is characterised by a high level of uncertainty.

If effects of gravitational and other geophysical processes are superposed, i.e. if torques, relative angular momenta and further deviations of the tensor of inertia are regarded in the Liouville equation, an interaction between forced and free oscillation occurs due to rotational deformations. While the impacts on the Chandler frequency are negligible (Okubo 1982; Jochmann 2003), the Chandler amplitude is strongly affected by the excitations (see Sect. 6.2).

Table 6.1 Periods and quality factors Q (with 90% confidence interval) of the Chandler oscillation from different studies

Chandler period	Q	[Interval]	Source
434.0 ± 2.5 days	100	[50, 400]	Wilson and Haubrich (1976)
431.7 days	24		Lenhardt and Groten (1985)
433.3 ± 3.6 days	179	[47, >1,000]	Wilson and Vicente (1990)
439.5 ± 1.2 days	72	[30, 500]	Kuehne et al. (1996)
433.7 ± 1.8 days	49	[35, 100]	Furuya and Chao (1996)
413 – 439 days			Schuh et al. (2001)
434.1 days	69		Seitz and Kutterer (2005)

6.4.2.2 Deformations Due to Surface Loads

Various processes in the subsystems of the Earth, such as the motion of atmospheric high-pressure and low-pressure systems, ocean bottom pressure changes or hydrologic variations over the continents due to flooding and snow, exert time-variable surface mass loads on the solid Earth. In this way they cause deformations of the Earth's body which are up to few centimetres in the vertical and several millimetres in the horizontal (Rabbel and Zschau 1985; Sun et al. 1995). The change of the surface geometry entails the redistribution of mass elements within the solid Earth which has a significant effect on both the Earth's gravity potential and its rotation. Consequently expedient information about atmosphere loading (van Dam and Herring 1994), non-tidal ocean loading (van Dam et al. 1997) and continental water storage variations (van Dam et al. 2001; Schuh et al. 2004) is required for an advanced interpretation and analysis of space geodetic observations (Rabbel and Schuh 1986; Manabe et al. 1991; Haas et al. 1997; Boehm et al. 2009). The surface forces exerted by time-variable mass distributions are in contrast to gravitationally induced body forces. While the latter cause large-scale and very regular deformations of the Earth that are well predictable, the effects of surface mass loads are mostly restricted to a few 100 km. Since they are irregular, they are hardly predictable (van Dam et al. 1997).

Vertical surface deformations of the solid Earth are usually computed following the theory of Farrell (1972). Pressure variations $p(\lambda, \varphi)$ (units of [Pa]) are related to time-variable surface mass loads $q(\lambda, \varphi)$ (units of [kg/m^2]) by

$$q(\lambda, \varphi) = \frac{p(\lambda, \varphi)}{g} \,, \tag{28}$$

where g is the gravitational acceleration. The radial displacement $d_\mathrm{r}(P)$ of the Earth at a position $P(\varphi_P, \lambda_P)$ caused by surface mass loads q_Q at locations $Q(\varphi_Q, \lambda_Q)$ on the Earth's surface area σ_Q is estimated by (Moritz and Mueller 1987)

$$d_\mathrm{r}(P) = \frac{a^3}{M} \iint\limits_{\sigma_Q} q_Q \sum_{n=0}^{\infty} h'_n P_n(\cos \psi_{PQ}) \, \mathrm{d}\sigma_Q \,. \tag{29}$$

In this equation h'_n denotes the degree n load Love number. The spherical distance between P and the location $Q(\varphi_Q, \lambda_Q)$ of an individual (point-)mass load is given by ψ_{PQ} which is the argument of the degree n Legendre Polynomial $P_n(\cos \psi_{PQ})$. More compact (29) can be written as

$$d_\mathrm{r}\,(P) = a^2 \iint\limits_{\sigma_Q} q_Q G\left(\psi_{PQ}\right) \, \mathrm{d}\sigma_Q \,, \tag{30}$$

where the abbreviation

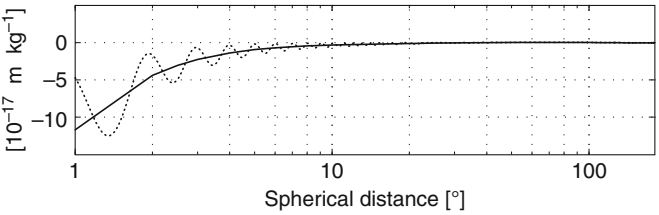

Fig. 6.7 Green's function $G\left(\psi_{PQ}\right)$ for the Earth model PREM. Dotted: truncation of the spherical harmonic expansion at degree $n = 350$, solid: infinite expansion

$$G\left(\psi_{PQ}\right) = \frac{a}{M} \sum_{n=0}^{\infty} h'_n P_n \left(\cos \psi_{PQ}\right) \tag{31}$$

is the Green's function for the vertical displacement (Farrell 1972). Function $G(\psi_{PQ})$ acts as a weighting operator which relates an individual surface mass load to the associated deformation of the solid Earth according to the spherical distance. Figure 6.7 shows the Green's function for continental crust computed from load Love numbers based on the previously mentioned Earth model PREM (Dziewonski and Anderson 1981; Scherneck 1990). The strong variability of the dotted curve truncated at $n = 350$ reflects the truncation error.

Figure 6.8 shows the time-variable deformations of the solid Earth for a period of two weeks in February 1994 as caused by atmosphere loading, non-tidal ocean loading and water storage variations over the continents (Seitz 2004). For the atmosphere and the ocean fields of surface mass loads $q_Q(\varphi_Q, \lambda_Q)$ were computed from a consistent combination of atmosphere surface pressure variations from reanalysis at the National Centers for Environmental Prediction/National Center for Atmospheric Research (NCEP/NCAR) (Kalnay et al. 1996) and ocean bottom pressure variations from the constrained version kf049f of the global ocean circulation model ECCO (Fukumori 2002). Outputs of both models are provided in daily intervals; spatial resolutions are 2.5° × 2.5° for NCEP/NCAR (globally) and 1° × 1° for ECCO (between 70° N/S; densification of the grid around the equator). Since atmosphere pressure forcing is not taken into account by ECCO, an inverse barometric correction is applied to the NCEP/NCAR fields, i.e. air pressure is set to zero over the ocean. Variations of continental hydrology are taken from the land dynamics model (LaD; version *Euphrates*) (Milly and Shmakin 2002). LaD data comprehends monthly values of global water and groundwater storage as well as snow loads per 1° × 1° grid cell. While the deformations over the continents are up to 2 cm, the influence of ocean bottom pressure variations on the surface geometry of the Earth is marginal.

In order to assess the effect of the deformations on Earth rotation, the vertical surface displacements have to be transformed into variations of the tensor of inertia $\Delta\underline{\mathbf{I}}(t)$. Since this two-step procedure, i.e. the computation of global load deformations and the subsequent transformation of the deformations into deviations

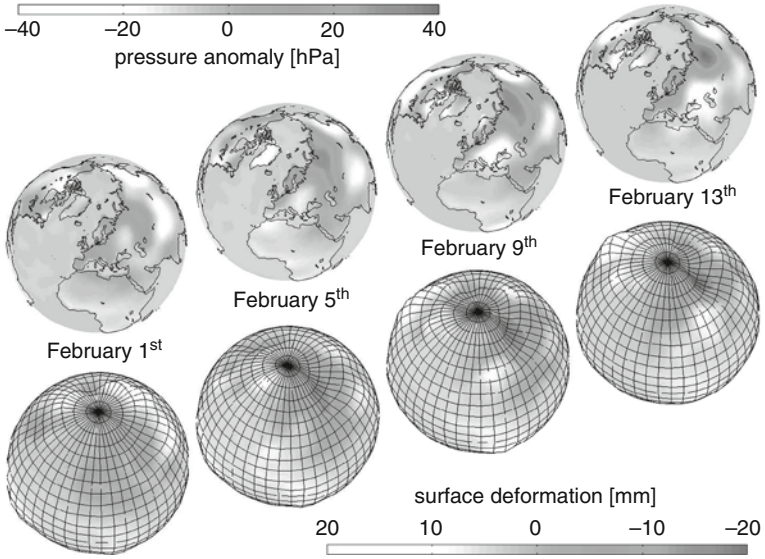

Fig. 6.8 Deformations of the solid Earth due to anomalies of atmospheric surface pressure, ocean bottom pressure, and continental water storage (Seitz 2004)

of the tensor of inertia (Dill 2002; Seitz 2004), is laborious and time-consuming, the indirect effect of mass redistributions on Earth rotation is commonly computed from changes of the geopotential associated with the mass load and the surface deformation.

The variation ΔU_{def} of the Earth's gravity potential U due to a surface deformation is proportional to the perturbing potential u of the surface mass load. The proportionality factor is the potential Love number k' (Moritz and Mueller 1987):

$$\Delta U_{\mathrm{def}} = k' u \; . \tag{32}$$

In general, the gravity potential u of a loading (point-)-mass m equals (Heiskanen and Moritz 1967)

$$u = \frac{Gm}{l} = \frac{Gm}{a} \sum_{n=0}^{\infty} \left(\frac{a - d_{\mathrm{r}}}{a} \right)^n P_n(\cos \psi_{PQ}) \; , \tag{33}$$

or, since the vertical deformation d_{r} is small compared to the Earth radius a:

$$u = \frac{Gm}{a} \sum_{n=0}^{\infty} P_n(\cos \psi_{PQ}) \; . \tag{34}$$

According to (32), the related change of the geopotential due to the induced surface deformation is

$$\delta U_{\mathrm{def}} = \frac{Gm}{a} \sum_{n=0}^{\infty} k'_n P_n(\cos \psi_{PQ}) \,. \tag{35}$$

If the point mass m is substituted by the (global) surface mass load q_Q, this equation turns into

$$\delta U_{\mathrm{def}} = Ga \iint_{\sigma_Q} q_Q \sum_{n=0}^{\infty} k'_n P_n(\cos \psi_{PQ}) \, \mathrm{d}\sigma_Q \,, \tag{36}$$

and the gravity potential u of the loading mass is

$$u = Ga \iint_{\sigma_Q} q_Q \sum_{n=0}^{\infty} P_n(\cos \psi_{PQ}) \, \mathrm{d}\sigma_Q \,. \tag{37}$$

Following the derivation given by Moritz and Mueller (1987), (37) can be written as

$$u = Ga \sum_{n=0}^{\infty} \frac{4\pi}{2n+1} q_{Qn} \,, \tag{38}$$

where q_{Qn} is the Laplace surface harmonic of degree n of the function q_Q, i.e.

$$q_Q = \sum_{n=0}^{\infty} q_{Qn} \,. \tag{39}$$

If accordingly the Laplace surface harmonic u_n of function u is introduced, the gravity potential of degree n of the surface mass load can be written as

$$u_n = Ga \frac{4\pi}{2n+1} q_{Qn} \,. \tag{40}$$

Since the variations of the tensor of inertia $\Delta \underline{\mathbf{I}}(t)$ are solely related to potential variations of degree 2 (Rochester and Smylie 1974; Chen et al. 2005; see also (22)), it is sufficient to evaluate (40) for $n = 2$. The temporal variation of $\delta U_2(t)$ due to the surface deformation is

$$\delta U_2(t) = k'_2 Ga \frac{4\pi}{5} q_{Q_2} \tag{41}$$

with $k'_2 = -0.308$ (Dong et al. 1996). The relation between the spherical harmonic coefficients of degree 2 and the elements of the Earth tensor of inertia is linear (Chen et al. 2005). Therefore tensor variations due to the indirect effect $\Delta \underline{\mathbf{I}}_{\mathrm{def}}(t)$ are computed simply by multiplying the direct tensor variations by the load Love number k'_2:

$$\Delta\underline{\mathbf{I}}_{\mathrm{def}}(t) = k'_2 \cdot \Delta\widehat{\underline{\mathbf{I}}}(t)\,, \tag{42}$$

where $\Delta\widehat{\underline{\mathbf{I}}}(t)$ denotes the direct tensor variations due to the mass redistributions within atmosphere, ocean and other subsystems that are causative for the Earth's surface deformations.

Given the above, the total (direct and indirect) effect of mass redistributions on the Earth's tensor of inertia is (Barnes et al. 1983)

$$\Delta\underline{\mathbf{I}}(t) = (1 + k'_2) \cdot \Delta\widehat{\underline{\mathbf{I}}}(t)\,. \tag{43}$$

Thus, the direct effect is attenuated by about 30% due to the deformation of the solid Earth. Note that this is only valid for mass redistributions that actually load the Earth's surface. For processes that are not accompanied by surface deformations (e.g. mass redistributions in the mantle) the load Love number k'_2 must be set to zero in this equation (Gross 2007).

6.4.3 Solution of the Euler–Liouville Equation

In order to compute variations of Earth rotation from angular momentum changes and torques, the Liouville equation (12) has to be solved for the unknown quantities $m_i(t)$ of the Earth rotation vector $\boldsymbol{\omega}(t)$. In general two different approaches, an analytical and a numerical approach, are applicable for the solution of the coupled system of the three first-order differential equations. Both methods will be discussed in the following.

Less compact the Liouville equation (12) can be written as

$$\dot{\underline{\mathbf{I}}}\,\boldsymbol{\omega} \;+\; \underline{\mathbf{I}}\,\dot{\boldsymbol{\omega}} \;+\; \dot{\mathbf{h}} \;+\; \boldsymbol{\omega} \times \underline{\mathbf{I}}\,\boldsymbol{\omega} \;+\; \boldsymbol{\omega} \times \mathbf{h} \;=\; \mathbf{L}\,, \tag{44}$$

where the dot denotes the derivative with respect to time. The individual terms read explicitly

$$\dot{\underline{\mathbf{I}}}\,\boldsymbol{\omega} \;=\; \begin{pmatrix} \dot{c}_{11} & \dot{c}_{12} & \dot{c}_{13} \\ \dot{c}_{12} & \dot{c}_{22} & \dot{c}_{23} \\ \dot{c}_{13} & \dot{c}_{23} & \dot{c}_{33} \end{pmatrix} \cdot \Omega \begin{pmatrix} m_1 \\ m_2 \\ 1 + m_3 \end{pmatrix}\,, \tag{45}$$

$$\underline{\mathbf{I}}\,\dot{\boldsymbol{\omega}} \;=\; \begin{pmatrix} A + c_{11} & c_{12} & c_{13} \\ c_{12} & B + c_{22} & c_{23} \\ c_{13} & c_{23} & C + c_{33} \end{pmatrix} \cdot \Omega \begin{pmatrix} \dot{m}_1 \\ \dot{m}_2 \\ \dot{m}_3 \end{pmatrix}\,, \tag{46}$$

$$\dot{\mathbf{h}} \;=\; \begin{pmatrix} \dot{h}_1 \\ \dot{h}_2 \\ \dot{h}_3 \end{pmatrix}\,, \tag{47}$$

$$\boldsymbol{\omega} \times \underline{\mathbf{I}}\,\boldsymbol{\omega} \;=\; \Omega \begin{pmatrix} m_1 \\ m_2 \\ 1 + m_3 \end{pmatrix} \times \begin{pmatrix} A + c_{11} & c_{12} & c_{13} \\ c_{12} & B + c_{22} & c_{23} \\ c_{13} & c_{23} & C + c_{33} \end{pmatrix} \cdot \Omega \begin{pmatrix} m_1 \\ m_2 \\ 1 + m_3 \end{pmatrix}\,, \tag{48}$$

$$\boldsymbol{\omega} \times \mathbf{h} \;=\; \Omega \begin{pmatrix} m_1 \\ m_2 \\ 1 + m_3 \end{pmatrix} \times \begin{pmatrix} h_1 \\ h_2 \\ h_3 \end{pmatrix} . \tag{49}$$

The traditionally applied analytical approach has been described and discussed in various publications (e.g. Munk and MacDonald 1960; Lambeck 1980; Wahr 1982; Barnes et al. 1983; Moritz and Mueller 1987; Gross 2007). Therefore only its basic principle shall be sketched in the following. In the numerical ansatz, the non-linear equation system is solved directly via numerical integration.

6.4.3.1 Linear Analytical Approach

In order to allow for a closed solution of the coupled system of differential equations (44), the following simplifications are commonly introduced (Lambeck 1980):

- With adequate accuracy, the Earth can be viewed as a biaxial, i.e. rotationally symmetric, body, so that the principal components A and B can be substituted by their average value $A' = (A + B)/2$. (Indeed the quotient of the difference between A and B and the absolute value of either of them amounts to only 2.2×10^{-5}; see Gross 2007.)
- Terms that contain products of the small quantities $m_i(t), c_{ij}(t)$ and $h_i(t)$ or their derivatives with respect to time are negligible (linearisation).

With these assumptions, the expansion of the expressions (45), (46), (48) and (49) results in

$$\dot{\underline{\mathbf{I}}}\,\boldsymbol{\omega} \;=\; \Omega \begin{pmatrix} \dot{c}_{13} \\ \dot{c}_{23} \\ \dot{c}_{33} \end{pmatrix} , \tag{50}$$

$$\underline{\mathbf{I}}\,\dot{\boldsymbol{\omega}} \;=\; \Omega \begin{pmatrix} A' \dot{m}_1 \\ A' \dot{m}_2 \\ C \dot{m}_3 \end{pmatrix} , \tag{51}$$

$$\boldsymbol{\omega} \times \underline{\mathbf{I}}\,\boldsymbol{\omega} \;=\; \Omega^2 \begin{pmatrix} m_2(C - A') - c_{23} \\ -m_1(C - A') + c_{13} \\ 0 \end{pmatrix} , \tag{52}$$

$$\boldsymbol{\omega} \times \mathbf{h} \;=\; \Omega \begin{pmatrix} -h_2 \\ h_1 \\ 0 \end{pmatrix} . \tag{53}$$

Insertion into the Liouville equation (44) yields

$$\begin{aligned}\Omega\begin{pmatrix}\dot{c}_{13}\\ \dot{c}_{23}\\ \dot{c}_{33}\end{pmatrix}+\Omega\begin{pmatrix}A'\,\dot{m}_1\\ A'\,\dot{m}_2\\ C\,\dot{m}_3\end{pmatrix}+\begin{pmatrix}\dot{h}_1\\ \dot{h}_2\\ \dot{h}_3\end{pmatrix}\\ +\Omega^2\begin{pmatrix}m_2(C-A')-c_{23}\\ -m_1(C-A')+c_{13}\\ 0\end{pmatrix}+\Omega\begin{pmatrix}-h_2\\ h_1\\ 0\end{pmatrix}=\begin{pmatrix}L_1\\ L_2\\ 0\end{pmatrix},\end{aligned}\tag{54}$$

or component-by-component

$$\dot{m}_1\cdot\frac{A'}{\Omega(C-A')}+m_2=\frac{1}{\Omega^2(C-A')}\cdot\left[L_1+\Omega^2c_{23}-\Omega\dot{c}_{13}+\Omega h_2-\dot{h}_1\right]\;=:\;\Psi_2\,,\tag{55}$$

$$\dot{m}_2\cdot\frac{A'}{\Omega(C-A')}-m_1\;=\frac{1}{\Omega^2(C-A')}\cdot\left[L_2-\Omega^2c_{13}-\Omega\dot{c}_{23}-\Omega h_1-\dot{h}_2\right]\;=:\;-\Psi_1\,,$$

$$\dot{m}_3=\frac{1}{\Omega C}\cdot\left[-\Omega\dot{c}_{33}-\dot{h}_3\right]\;=:\;\dot{\Psi}_3\,.\tag{57}$$

The terms containing the time-variable equatorial components of the external torques $L_1(t)$ and $L_2(t)$ as well as the quantities $c_{ij}(t), h_i(t)$ or their derivatives with respect to time are referred to as *excitation functions* $\Psi_i\,(i=1,2,3)$ (Munk and MacDonald 1960). Note that $L_3=0$ due to $A=B$; see (18). Variations of the tensor elements $c_{13}(t), c_{23}(t)$ and $c_{33}(t)$ describe the sum of all direct effects of mass redistributions in the various system components and the effects of solid Earth deformations due to tides, polar motion and surface loads. For the principal moments of inertia A' and C numerical values have to be introduced that account for the effect of core–mantle decoupling as discussed in Sect. 6.4.2.1.

Due to the linearisation, only three of the six components of the tensor of inertia appear in the excitation functions. Deviation moments $c_{11}(t), c_{22}(t)$ and $c_{12}(t)$ are neglected in the analytical approach. The axial component $m_3(t)$ of the Earth rotation vector $\boldsymbol{\omega}(t)$ is decoupled from the horizontal components. With adequate accuracy $\Delta\mathrm{LOD}(t)$ can be calculated independently from polar motion (see (15)). For the computation of polar motion, the first two differential equations are transformed into a complex equation (Lambeck 1980). Defining $m(t)=m_1(t)+im_2(t)$ and $\Psi(t)=\Psi_1(t)+i\Psi_2(t)$ yields

$$i\cdot\left(\dot{m}\frac{A'}{\Omega(C-A')}\right)+m=\Psi\,,\tag{58}$$

where $i=\sqrt{-1}$. For a rigid body and in the absence of external torques Ψ equals zero. Then the solution of (58) is

$$m=m^0e^{i\sigma t}\,,\tag{59}$$

with the abbreviation $\sigma = \Omega \frac{(C - A')}{A'}$ and the complex coordinate $m^0 = m(t_0)$ as initial condition for the epoch t_0. The free polar motion of a rigid Earth would be a prograde and undamped oscillation with amplitude $|m^0|$ and frequency σ, which corresponds to a period of 304 days (Euler period).

The observed frequency of the free polar motion (Chandler frequency) differs from the Euler frequency due to the deformability of the Earth's body. As a consequence of mantle anelasticity, rotational deformations are accompanied by a loss of energy due to friction (see Sect. 6.4.2.1). In order to account for this effect, σ is substituted by the complex quantity σ_{CW} (Lambeck 1980):

$$\sigma_{\mathrm{CW}} = \sigma_0 \left(1 + \frac{i}{2Q}\right). \tag{60}$$

Here σ_0 is the Chandler frequency and Q denotes the quality factor that describes the damping of the Chandler amplitude due to dissipation. Both quantities are explicitly predetermined in the analytical approach. Therefore the result is directly dependent on the choice of the numerical values of σ_0 and Q (Wilson and Haubrich 1976). Due to the assumption of rotational symmetry ($A = B$), the resulting free polar motion is circular. For a deformable Earth the solution of the Liouville equation follows from the convolution

$$m = e^{i\sigma_{\mathrm{CW}} t} \left[m^0 - i\sigma_{CW} \int_{-\infty}^{t} \Psi(\tau) e^{-i\sigma_{\mathrm{CW}} \tau} \mathrm{d}\tau \right]. \tag{61}$$

Alternative to the explicit computation of polar motion from the excitation functions $\Psi_1(t)$ and $\Psi_2(t)$, an indirect method is commonly applied, in which the so-called *geodetic excitation* is derived by an inverse convolution from the observed polar motion (Chao 1985; Brzezinski 1992). The comparison between the gravitational and geophysical processes and the geodetic observations is then performed on the basis of the excitation functions $\Psi_1(t)$ and $\Psi_2(t)$ without calculating $m_1(t)$ and $m_2(t)$. Since the Chandler oscillation is a priori reduced from the observations in the course of the computation of the geodetic excitation, the indirect method is just like the direct method dependent on the choice of the parameters σ_0 and Q.

6.4.3.2 Non-linear Numerical Approach

In the non-linear numerical approach the system of the three differential equations (44) is solved numerically. In contrast to the analytical approach, the Chandler oscillation is not explicitly predetermined with respect to its period σ_0 and quality factor Q. Instead, the free polar motion is modelled by considering the effect of the back-coupling mechanism of rotational deformations in $\Delta \underline{\mathbf{I}}(t)$. As described in Sect. 6.4.2.1, frequency and damping of the Chandler oscillation are closely related to the value of the complex Love-number k_2 in this case (Seitz and Kutterer 2005).

No set-up of linearised excitation functions is required when the system of differential equations is solved numerically. This is a major difference compared to the

analytical approach: the tensor of inertia $\underline{\mathbf{I}}(t)$, the vector of angular momenta $\mathbf{h}(t)$ and the vector of the external torques $\mathbf{L}(t)$ are directly introduced into the Liouville equation. Therefore the temporal variations of the deviation moments c_{11}, c_{22} and c_{12} are also considered in the tensor of inertia, and the previously neglected higher-order terms are contained in the solution. As a consequence, the first two differential equations are not decoupled from the third one, i.e. polar motion and ΔLOD(t) are solved simultaneously.

Furthermore the numerical approach allows for the introduction of a triaxial approximate tensor $\underline{\mathbf{I}}_0(A \neq B \neq C)$. The free polar motion of such an unsymmetrical gyro is no longer circular. But since the discrepancy between A and B is small, the numerical eccentricity of the ellipse described by the Earth rotation vector with respect to the Earth-fixed reference frame is only 0.10 if all gravitational and geophysical excitations are neglected. Its semi-minor axis is oriented towards the direction of the smallest principal moment of inertia A.

The Liouville equation is reformulated as a coupled system of three ordinary differential equations of the general form

$$\dot{\mathbf{m}}(t) = f\left(t, m_i(t)\right) , \tag{62}$$

$(i = 1, 2, 3)$ with

$$\dot{\mathbf{m}}(t) = \begin{pmatrix} \dot{m}_1(t) \\ \dot{m}_2(t) \\ \dot{m}_3(t) \end{pmatrix} , \tag{63}$$

and

$$f(t, m_i(t)) = \begin{pmatrix} f_1(t, m_1(t), m_2(t), m_3(t)) \\ f_2(t, m_1(t), m_2(t), m_3(t)) \\ f_3(t, m_1(t), m_2(t), m_3(t)) \end{pmatrix} . \tag{64}$$

Function $f(t, m_i(t))$ comprehends the tensor of inertia $\underline{\mathbf{I}}(t)$, relative angular momenta $\mathbf{h}(t)$ and torques $\mathbf{L}(t)$. Due to rotational deformations, the tensor of inertia includes deviations, which are dependent on m_1 and m_2 (cf. (21) and (22)). Consequently derivatives of these parameters with respect to time $\dot{m}_i$ appear in both terms $\underline{\mathbf{I}}\ \dot{\boldsymbol{\omega}}$ and $\dot{\underline{\mathbf{I}}}\ \boldsymbol{\omega}$ of the Liouville equation (44). In order to solve the Liouville equation for the unknown quantities m_i, their derivatives are assembled on the left-hand side of the differential equation. Therefore the tensor of inertia $\dot{\underline{\mathbf{I}}}$ is divided into two parts: one component, $\dot{\underline{\mathbf{I}}}_{\mathrm{R}}$, describes the effect of rotational deformations and depends on $\dot{m}_i$; the second component $\dot{\underline{\mathbf{I}}}_{\mathrm{G}}$ includes the geophysically induced mass redistributions in the fluid system components and in the solid Earth due to tidal deformations and load deformations. This second component $\dot{\underline{\mathbf{I}}}_{\mathrm{G}}$ is independent of $\dot{m}_i$. Consequently the Liouville equation can be written as

$$\dot{\underline{\mathbf{I}}}_{\mathrm{R}}\ \boldsymbol{\omega} + \underline{\mathbf{I}}\ \dot{\boldsymbol{\omega}} = \mathbf{L} - \dot{\underline{\mathbf{I}}}_{\mathrm{G}}\ \boldsymbol{\omega} - \dot{\mathbf{h}} - \boldsymbol{\omega} \times \mathbf{h} - \boldsymbol{\omega} \times \underline{\mathbf{I}}\ \boldsymbol{\omega} . \tag{65}$$

If the products of the m_i with the (very small) derivatives $\dot{m}_i$ are neglected, the term $\dot{\underline{\mathbf{I}}}_{\mathrm{R}}\,\boldsymbol{\omega}$ equals

$$\dot{\underline{\mathbf{I}}}_{\mathrm{R}}\,\boldsymbol{\omega} \;=\; \frac{\Omega^3 a^5}{3G}\begin{bmatrix} \Re(k_2)\cdot\dot{m}_1 + \Im(k_2)\cdot\dot{m}_2 \\ \Re(k_2)\cdot\dot{m}_2 - \Im(k_2)\cdot\dot{m}_1 \\ 0 \end{bmatrix} \tag{66}$$

$$\approx \frac{\Omega^3 a^5}{3G}\Re(k_2)\begin{bmatrix} \dot{m}_1 \\ \dot{m}_2 \\ 0 \end{bmatrix}. \tag{67}$$

Since the real part of k_2 is two orders of magnitude larger than its imaginary part, the products of $\Im(k_2)$ with $\dot{m}_i$ are neglected, too. The left-hand side of system (65) turns into

$$\dot{\underline{\mathbf{I}}}_{\mathrm{R}}\,\boldsymbol{\omega} \;+\; \underline{\mathbf{I}}\,\dot{\boldsymbol{\omega}} = \left(\frac{\Omega^3 a^5}{3G}\Re(k_2)\begin{bmatrix} 1&0&0\\0&1&0\\0&0&0 \end{bmatrix} + \Omega\,\underline{\mathbf{I}}\right)\begin{bmatrix} \dot{m}_1 \\ \dot{m}_2 \\ \dot{m}_3 \end{bmatrix} \tag{68}$$

$$=: \underline{\mathbf{F}}\begin{bmatrix} \dot{m}_1 \\ \dot{m}_2 \\ \dot{m}_3 \end{bmatrix}, \tag{69}$$

and the Liouville equation can be converted into

$$\dot{\mathbf{m}} = \underline{\mathbf{F}}^{-1}\left(\mathbf{L} \;-\; \dot{\underline{\mathbf{I}}}_{\mathrm{G}}\,\boldsymbol{\omega} \;-\; \dot{\mathbf{h}} \;-\; \boldsymbol{\omega}\times\mathbf{h} \;-\; \boldsymbol{\omega}\times\underline{\mathbf{I}}\,\boldsymbol{\omega}\right). \tag{70}$$

This coupled system of three first-order differential equations is solved as an initial value problem. Just as in the analytical approach, the tensor of inertia is composed of all contributions from direct mass effects in the components of the Earth system and from the deformations of the solid Earth induced by tides, polar motion and loading. The effect of core–mantle decoupling is regarded by the adoption of appropriate values of the principal moments of inertia A, B, C; see Sect. 6.4.2.1.

The introduction of initial values for the epoch t_0

$$\mathbf{m^0} = \begin{pmatrix} m_1^0 \\ m_2^0 \\ m_3^0 \end{pmatrix} \tag{71}$$

allows for a unique computation of special solutions for the unknown functions $m_i = m_i(t)$ by which the initial conditions $m_i(t_0) = m_i^0$ are fulfilled. Respective values m_i^0 are deduced from observations of polar motion and ΔLOD. For the correspondence between the geodetic observations and the quantities $m_i(t)$, see Sect. 6.5.

The efficiency of the numerical solution is naturally linked to the quality of both the applied initial conditions and the integrator. Using the previously mentioned dynamic Earth system model (see Sect. 6.4.2.1), Seitz and Kutterer (2005)

studied the effect of inaccurate initial values on the numerical solution. They concluded from 30 test runs that the variation of the initial values within an interval of $\pm 3\sigma_i$ (where σ_i is the standard deviation of the respective observation) is uncritical. However, if the applied initial values differ substantially from the geodetic observations (e.g. if $m_i^0 = 0$ is assumed), the results are contaminated over many decades. In this case the model time series are not interpretable before a steady state is reached, i.e. before the influence of the initial conditions falls below the level of the model accuracy. Studies on the reliability of the solution from an algorithmic point of view showed little dependence of the results on the choice of a specific solver: Seitz (2004) applied various one-step and multi-step solvers as well as an extrapolation method in the dynamic Earth system model and performed runs over more than two decades with identical initial values and forcing conditions. It was shown that the RMS differences between all runs were in the order of 1 mas for polar motion and 1–2 μs for ΔLOD. In contrast, the absolute accuracy of the model, i.e. the RMS difference between the simulation and the geodetic observations, was in the order of 30 mas for polar motion and 120 μs for ΔLOD.

More details on the non-linear approach, numerical model results from the dynamic Earth system model and comparisons between modelled and observed time series for polar motion and ΔLOD can be found in Seitz (2004) and Seitz and Schmidt (2005).

6.5 Relation Between Modelled and Observed Variations of Earth Rotation

The parameters $m_i(t)$ of the Earth rotation vector $\boldsymbol{\omega}(t)$ in the Liouville Equation (12) are related to the geodetically observed time series of polar motion $[x_\mathrm{p}(t), y_\mathrm{p}(t)]$, $\Delta\mathrm{UT}(t)$ and length-of-day variations $\Delta\mathrm{LOD}(t)$. The time-variable angular misalignment between the instantaneous rotation vector $\boldsymbol{\omega}(t)$ and the z-axis of the terrestrial reference frame in x- and y-direction is described by the two components $m_1(t)$ and $m_2(t)$, respectively (see (14)). On the other hand, the coordinates x_p and y_p published by the IERS represent the misalignment between the CIP and the IERS Reference Pole (i.e. the z-axis of the ITRF).

Both coordinate systems differ with respect to the direction of the positive y-axis: the terrestrial system, to which the rotation vector $\boldsymbol{\omega}(t)$ refers to, is a right-hand system. The system used by the IERS for the publication of the coordinates $x_\mathrm{p}(t)$ and $y_\mathrm{p}(t)$, however, is a left-hand system (y_p-axis directed towards 90°W; see Sect. 6.1). Therefore the coordinates $[p_1(t), p_2(t)]$ are defined, in order to describe the position of the CIP with respect to the IERS Reference Pole in a right-hand system:

$$\begin{aligned} p_1(t) &= x_\mathrm{p}(t)\,, \\ p_2(t) &= -y_\mathrm{p}(t)\,. \end{aligned} \tag{72}$$

The relation between $[m_1(t), m_2(t)]$ and $[p_1(t), p_2(t)]$ follows from the transformation between the true celestial equator system and the Earth-fixed system. According to Sect. 6.1, the rotation matrix $\underline{A}(t)$ that transforms between both systems accounts

for the daily spin around the axis of the CIP and polar motion:

$$\underline{A}(t) = \underline{W}(t)\, \underline{S}(t)\ . \tag{73}$$

The coordinates $\omega_1(t), \omega_2(t), \omega_3(t)$ of the Earth rotation vector $\boldsymbol{\omega}(t)$ in the terrestrial system are the elements of the skew-symmetric matrix $\underline{B}(t)$:

$$\underline{B}(t) = \begin{pmatrix} 0 & \omega_3(t) & -\omega_2(t) \\ -\omega_3(t) & 0 & \omega_1(t) \\ \omega_2(t) & -\omega_1(t) & 0 \end{pmatrix} = \dot{\underline{A}}(t)\underline{A}^{\mathrm{T}}(t)\ . \tag{74}$$

Since matrix $\underline{W}(t)$, and accordingly matrix $\underline{A}(t)$, do not include the previously mentioned Oppolzer motion, the Earth rotation vector $\boldsymbol{\omega}(t)$ resulting from (74) does not account for the subdaily retrograde deflection between the instantaneous rotation axis and the direction to the CIP. In order to include this effect, a vector that describes the departure between CIP and the instantaneous rotation pole (IRP) would have to be added to the product $\dot{\underline{A}}(t)\underline{A}^{\mathrm{T}}(t)$ (see below).

For time scales longer than 1 day, the comparison of the coefficients of matrix $\underline{B}(t)$ with the result of the product $\dot{\underline{A}}(t)\underline{A}^{\mathrm{T}}(t)$ leads to the relation between the elements of the Earth rotation vector $\boldsymbol{\omega}(t)$ and the coordinates $p_1(t)$ and $p_2(t)$. To the first order, this relation is (Brzezinski 1992; Gross 1992)

$$\begin{aligned} \omega_1(t) &= \Omega\, p_1(t) + \dot{p}_2(t)\,, \\ \omega_2(t) &= \Omega\, p_2(t) - \dot{p}_1(t)\,, \end{aligned} \tag{75}$$

or with $\omega_1(t) = \Omega\, m_1(t)$ and $\omega_2(t) = \Omega\, m_2(t)$

$$\begin{aligned} m_1(t) &= p_1(t) + \frac{1}{\Omega}\, \dot{p}_2(t)\,, \\ m_2(t) &= p_2(t) - \frac{1}{\Omega}\, \dot{p}_1(t)\ . \end{aligned} \tag{76}$$

The connection between modelled and observed polar motion is illustrated in Fig. 6.1 following Mendes Cerveira et al. (2009). The published polar motion values $p(t)$ refer to the position of the CIP in the ITRF, where $p(t) = x_p(t) - iy_p(t) = p_1(t) + ip_2(t)$. As stated above, the model values $m(t) = m_1(t) + im_2(t)$ represent polar motion of the IRP in the terrestrial frame that differs from the CIP by the effect of the Oppolzer motion (vector d in Fig. 6.1) (Capitaine 2002; Mendes Cerveira et al. 2009). For completeness, the axes of the space-fixed reference frame (GCRF) are also sketched. The coordinates $X(t)$ and $Y(t)$ of the CIP in the GCRF are derived from the precession–nutation (PN) model IAU 2000A and the published celestial pole offsets as described in Sect. 6.1.

The correspondence between the variation of the absolute value of the Earth rotation vector $\boldsymbol{\omega}(t)$ and the observed quantities $\Delta\mathrm{LOD}(t)$ and $\Delta\mathrm{UT}(t)$ results directly from the definition of $\Delta\mathrm{LOD}(t)$, meaning the time span of one full revolution of the Earth reduced by 86,400 s (see (5)):

$$\Delta \mathrm{LOD}\,(t) = \frac{2\,\pi\,\kappa}{|\boldsymbol{\omega}(t)|} - 86,400\,\mathrm{s}\,, \tag{77}$$

where

$$\kappa = \frac{\Omega}{2\,\pi} \cdot 86,400\,\mathrm{s} \quad = \quad \frac{86,400}{86,164}\,. \tag{78}$$

The introduction of the absolute value of $\boldsymbol{\omega}(t)$ (15) delivers (Schneider 1988)

$$\Delta \mathrm{LOD}\,t = \frac{2\,\pi\,\kappa}{\Omega(1 + m_3(t))} - 86,400\,\mathrm{s} \quad = \quad -m_3(t) \cdot 86,400\,\mathrm{s}\,, \tag{79}$$

and according to the relation between $\Delta\mathrm{LOD}\,(t)$ and $\Delta\mathrm{UT}\,(t)$ (6) (Gross 1992)

$$\frac{\mathrm{d}}{\mathrm{d}t}\Delta\mathrm{UT}\,(t) = m_3(t)\,. \tag{80}$$

Following the derivations in this section, physical model results and published values of Earth orientation parameters from space-geodetic observation techniques can be uniquely related to each other. In this way, physical models of Earth rotation can contribute significantly to the interpretation of the observations in terms of geophysical processes in the Earth system. Studies of the Earth's reaction on gravitational and other geophysical excitations, e.g. processes and interactions within and between atmosphere, hydrosphere and solid Earth can be performed using theoretical forward models. As described in Sect. 6.4, such models comprehend physical transfer functions that relate gravitational and geophysical model data and/or observations to time series of geodetic parameters of rotation, gravity field variations and changes of the surface geometry of the Earth. In forward models, observations of Earth rotation are used as a reference in order to examine the quality of geophysical data sets by balancing modelled angular momentum variations in the Earth's subsystems with the observed integral signal. Forward models have also been used for the prediction of geodetic parameters, e.g. in the context of global change, when climate predictions are introduced as forcing (Winkelnkemper et al. 2008).

Vice versa, observed time series of Earth orientation parameters can be used in order to support and improve theoretical models via inverse methods. In this way, the geodetic observations can contribute directly to an improved understanding of Earth system dynamics. Inverse methods have been developed for many years in geodesy. They are directed towards the gain of knowledge from precise geodetic observations about geophysical parameters (Marchenko and Schwintzer 2003), individual dynamic processes or interactions in the Earth system. While numerous recent studies deal with the assessment of the Earth's mass redistribution from an inversion of the time-variable gravity field from GRACE (Chao 2005; Ramillien et al. 2005), time series of geometric surface deformations from GPS (Wu et al. 2003) or combination of both (Wu et al. 2002; Kusche and Schrama 2005), there are hardly any approaches for the inversion of Earth rotation up to now. But due to the long observation records of polar motion and ΔLOD, due to the high accuracy

of the measurements and due to the large spectral range from hours to decades that is covered by the observations, the development of inverse Earth rotation models is a highly promising challenge for the future.

Acknowledgement The authors would like to express their gratitude to Urs Hugentobler from the Technische Universität München, Germany, and to Aleksander Brzezinski from the Polish Academy of Sciences, Warsaw, Poland, whose comments on the manuscript were very helpful and substantially improved the content of this chapter.

References

Altamimi, Z., Collilieux, X., Legrand, J., Garayt, B. and Boucher, C. (2007) ITRF2005: a new release of the International Terrestrial Reference Frame based on time series of station positions and Earth Orientation Parameters. J. Geophys. Res., 112, 10.1029/2007JB004949

Aoki, S., Guinot, B., Kaplan, G.H., Kinoshita, H., McCarthy, D.D. and Seidelmann, P.K. (1982) The new definition of universal time. Astron. Astrophys., 105, 359–361

Aoki, S. and Kinoshita, H. (1983) Note on the relation between the equinox and Guinot's nonrotating origin. Celest. Mech. Dyn. Astr., 29, 335–360

Barnes, R.T.H., Hide, R.H., White, A.A. and Wilson, C.A. (1983) Atmospheric angular momentum fluctuations, length of day changes and polar motion. Proc. R. Soc. Lon., 387, 31–73

Beutler, G. (2005) Methods of Celestial Mechanics I: Physical, Mathematical and Numerical Principles. Springer, Berlin

BIPM (2007) Director's Report on the Activity and Management of the International Bureau of Weights and Measures, Bureau International des Poids et Mesures, sévres Cedex

Bizouard, C. and Gambis, D. (2009) The combined solution C04 for Earth Orientation Parameters consistent with International Terrestrial Reference Frame 2005. In: Drewes, H. (ed) Geodetic Reference Frames. IAG Symposia 134, Springer, Berlin

Boehm, J., Heinkelmann, R., Mendes Cerveira, J.P., Pany, A. and Schuh, H. (2009) Atmospheric loading corrections at the observation level in VLBI analysis, J. Geodesy, 83, 1107–1113

Brzezinski, A. (1992) Polar motion excitation by variations of the effective angular momentum function: considerations concerning deconvolution problem. manuscripta geodaetica, 17, 3–20

Brzezinski, A. (2001) Diurnal and subdiurnal terms of nutation: a simple theoretical model for a nonrigid Earth. In: Capitaine, N. (ed) Proceedings of the Journées Systémes de Référence Spatiotemporels 2000, Paris, pp. 243–251

Brzezinski, A. and Nastula, J. (2000) Oceanic excitation of the Chandler wobble. Adv. Space Res., 30(2), 195–200

Capitaine, N. (2002) Comparison of 'old' and 'new' concepts: the Celestial Intermediate Pole and Earth orientation parameters. In: Capitatine, N., Gambis, D., McCarthy, D.D., Petit, G., Ray, J., Richter, B., Rothacher, M., Standish, E.M. and Vondrak, J. (eds) Proceedings of the IERS Workshop on the Implementation of the New IAU Resolutions, IERS Technical Note 29, Verlag des Bundesamts für Kartographie und Geodäsie, Frankfurt am Main, pp. 35–44

Capitaine, N. (2004) Oppolzer terms: a review, FGS Workshop on 'Ring Laser Gyroscopes and Earth Rotation', Wettzell

Capitaine, N. (2008) Definition and realization of the celestial intermediate reference system. Proc. IAU 2007, 3, 10.1017/S1743921308019583

Capitaine, N., Chapront, J., Lambert, S. and Wallace, P. (2002) Expressions for the coordinates of the CIP and the CEO Using IAU 2000 Precession-Nutation. In: Capitatine, N., Gambis, D., McCarthy, D.D., Petit, G., Ray, J., Richter, B., Rothacher, M., Standish, E.M. and Vondrak, J. (eds) Proceedings of the IERS Workshop on the Implementation of the New IAU Resolutions, IERS Technical Note 29, Verlag des Bundesamts für Kartographie und Geodäsie, Frankfurt am Main, pp. 89–91

Chandler, S.C. (1891) On the variation of latitude I-IV. Astron. J., 11, 59–61, 65–70, 75–79, 83–86
Chandler, S.C. (1892) On the variation of latitude V-VII. Astron. J., 12, 17–22, 57–72, 97–101
Chao, B.F. (1985) On the excitation of the Earth's polar motion. Geophys. Res. Lett., 12(8), 526–529
Chao, B.F. (1989) Length-of-day variations caused by El Nino Southern Oscillation and quasibiennial oscillation. Science, 243, 923–925
Chao, B.F. (1994) The geoid and Earth rotation. In: Vanićek, P. and Christou, N.T. (eds) Geoid and Its Geophysical Interpretations. CRC Press, Boca Raton, pp. 285–298
Chao, B.F. (2005) On inversion for mass distribution from global (time-variable) gravity field. J. Geodyn., 39(3), 223–230
Chao, B.F. and Gross, R.S. (1987) Changes in the Earth's rotation and low-degree gravitational field induced by earthquakes. Geophys. J. R. Astron. Soc., 91, 569–596
Chao, B.F. and Gross, R.S. (2005) Did the 26 December 2004 Sumatra, Indonesia, earthquake disrupt the Earth's rotation as the mass media have said? EOS Trans. Amer. Geophys. Union, 86, 1–2
Chen, J.L., Wilson, C.R. and Tapley, B.D. (2005) Interannual variability of low-degree gravitational change, 1980–2002. J. Geodesy, 78, 535–543
Dehant, V., Arias, F., Bizouard, C., Bretagnon, P., Brzezinski, A., Buffett, B., Capitaine, N., Defraigne, P., de Viron, O., Feissel, M., Fliegel, H., Forte, A., Gambis, D., Getino, J., Gross, R., Herring, T., Kinoshita, H., Klioner, S., Mathews, P., Mc-Carthy, D., Moisson, X., Petrov, S., Ponte, R., Roosbeek, F., Salstein, D., Schuh, H., Seidelmann, K., Soffel, M., Souchay, J., Vondrak, J., Wahr, J., Wallace, P., Weber, R., Williams, J., Yatskiv, Y., Zharov, V. and Zhu, S. (1999) Considerations concerning the non-rigid Earth nutation theory. Celest. Mech. Dyn. Astr., 72(4), 245–310
de Viron, O., Bizouard, C., Salstein, D. and Dehant, V. (1999) Atmospheric torque on the Earth and comparison with atmospheric angular momentum variations. J. Geophys. Res., 104, 4861–4875
de Viron, O. and Dehant, V. (2003a) Tests on the validity of atmospheric torques on Earth computed from atmospheric model outputs. J. Geophys. Res., 108, 10.1029/2001JB001196
de Viron, O. and Dehant, V. (2003b) Reliability of atmospheric torque for geodesy. In: Richter, B., Schwegmann, W. and Dick, W.R. (eds) Proceedings of the IERS Workshop on Combination Research and Global Geophysical Fluids, IERS Technical Note 30, Verlag des Bundesamts für Kartographie und Geodäsie, Frankfurt am Main, pp. 125–126
de Viron, O., Koot, L. and Dehant, V. (2005) Polar motion models: the torque approach. In: Plag, H.-P., Chao, B.F., Gross, R. and van Dam, T. (eds) Forcing of Polar Motion in the Chandler Frequency Band: A Contribution to Understanding Interannual Climate Variations, Cahiers du Centre Européen de Géodynamique et de Séismologie 24, Luxembourg
de Viron, O., Ponte, R.M. and Dehant, V. (2001) Indirect effect of the atmosphere through the oceans on the Earth nutation using the torque approach. J. Geophys. Res., 106, 8841–8851
Dill, R. (2002) Der Einfluss von Sekundäreffekten auf die Rotation der Erde, C 550, Deutsche Geodätische Kommission, München (in German)
Dong, D., Gross, R.S. and Dickey, J.O. (1996) Seasonal variations of the Earth's gravitational field: an analysis of atmospheric pressure, ocean tidal, and surface water excitation. Geophys. Res. Lett., 23(7), 725–728
Dziewonski, A.M. and Anderson, D.L. (1981) Preliminary Reference Earth model (PREM). Phys. Earth Planet. Int., 25, 297–356
Engels, J. and Grafarend, E.W. (1999) Zwei polare geodätische Bezugssysteme: Der Referenzrahmen der mittleren Oberflächenvortizität und der Tisserand-Referenzrahmen. In: Schneider, M. (ed) 3. DFG-Rundgespräch zum Thema Bezugssysteme. Mitteilungen des Bundesamts für Kartographie und Geodäsie, Verlag des Bundesamts für Kartographie und Geodäsie, Frankfurt am Main (in German), pp. 100–109
Euler, L. (1765) Du mouvement de rotation des corps solides autour d'un axe variable. Mémoires de l'académie des sciences de Berlin, 14, 154–193
Farrell, W. (1972) Deformation of the Earth by surface loads. Rev. Geophys. Space Phys., 10, 761–797

Feissel, M. and Mignard, F. (1998) The adoption of ICRS on 1 January 1998: meaning and consequences. Astron. Astrophys., 331, L33–L36
Fey, A.L., Ma, C., Arias, E.F., Charlot, P., Feissel-Vernier, M., Jacobs, A.M.G.C.S., Li, J. and MacMillan, D.S. (2004) The second extension of the International Celestial Reference Frame. Astron. J., 127, 3587–3608
Fricke, W., Schwan, H. and Lederle, T. (1988) Fifth Fundamental Catalogue, Part I., Techn. Ber., Veröff. Astron. Rechen Inst., Heidelberg
Fukumori, I. (2002) A partitioned Kalman filter and smoother. Mon. Weather Rev., 130, 1370–1383
Furuya, M. and Chao, B.F. (1996) Estimation of period and Q of the Chandler wobble. Geophys. J. Int., 127, 693–702
Furuya, M., Hamano, Y. and Naito, I. (1996) Quasi-periodic wind signal as a possible excitation of Chandler wobble. J. Geophys. Res., 101, 25537–25546
Gilbert, F. and Dziewonski, A.M. (1975) An application of normal mode theory to the retrieval of structural parameters and source mechanisms from seismic spectra. Phil. Trans. R. Soc., A278, 187–269
Gipson, J.M. and Ma, C. (1998) Site displacement due to variation in Earth rotation. J. Geophys. Res., 103, 7337–7350
Gontier, A.M., Arias, E.F. and Barache, C. (2006) Maintenance of the ICRF using the most stable sources. In: Souchay, J. and Feissel-Vernier, M. (eds) The International Celestial Reference System and Frame, 7–19, IERS Technical Note 34, Verlag des Bundesamts für Kartographie und Geodäsie, Frankfurt am Main
Gross, R.S. (1986) The influence of earthquakes on the Chandler wobble during 1977–1983. Geophys. J. R. Astr. Soc., 85, 161–177
Gross, R.S. (1992) Correspondence between theory and observations of polar motion. Geophys. J. Int., 109, 162–170
Gross, R.S. (1993) The effect of ocean tides on the Earth's rotation as predicted by the results of an ocean tide model. Geophys. Res. Lett., 20(4), 293–296
Gross, R.S. (2000) The excitation of the Chandler wobble. Geophys. Res. Lett., 27(15), 2329–2332
Gross, R.S. (2007) Earth rotation variations – Long period. In: Herring, T.A. (ed) Physical Geodesy, Treatise on Geophysics, Vol. 3. Elsevier, Amsterdam
Guinot, B. (1979) Basic problems in the kinematics of the rotation of the earth. In: McCarthy, D. and Pilkington, J. (eds) Time and the Earth's Rotation. D. Reidel, Dordrecht, pp. 7–18
Guinot, B. (2002) Comparison of 'old' and 'new' concepts: Celestial Ephemeris Origin (CEO), Terrestrial Ephemeris Origin (TEO), Earth Rotation Angle (ERA). In: Capitatine, N., Gambis, D., McCarthy, D.D., Petit, G., Ray, J., Richter, B., Rothacher, M., Standish, E.M. and Vondrak, J. (eds) Proceedings of the IERS Workshop on the Implementation of the New IAU Resolutions, IERS Technical Note 29, Verlag des Bundesamts für Kartographie und Geodäsie, Frankfurt am Main, pp. 45–50
Haas, R., Scherneck, H.-G. and Schuh, H. (1997) Atmospheric loading corrections in geodetic VLBI and determination of atmospheric loading coefficients. In: Pettersen, B.R. (ed) Proceedings of the 12th Working Meeting on European VLBI for Geodesy and Astronomy, Statens Kartverk, Hønefoss, pp. 111–121
Hameed, S. and Currie, R.G. (1989) Simulation of the 14-month Chandler wobble climate model. Geophys. Res. Lett., 16(3), 247–250
Heiskanen, W.A. and Moritz, H. (1967) Physical Geodesy. Freeman and Co., San Francisco
Hinderer, J., Legros, H., Gire, C. and Le Mouël, J.-L. (1987) Geomagnetic secular variation, core motions and implications for the Earth's wobbles. Phys. Earth Planet. Int., 49, 121–132
Holme, R. (1998) Electromagnetic core-mantle coupling – I. Explaining decadal changes in length of day. Geophys. J. Int., 132, 167–180
Höpfner, J. (2001) Interannual variations in length of day and atmospheric angular momentum with respect to ENSO cycles. Zeitschrift f. Vermessungswesen, 126(1), 39–49
IERS (2008) IERS Annual Report 2006. In: Dick, W.R. und Richter, B. (Hrsg.) Verlag des Bundesamts für Kartographie und Geodäsie, Frankfurt am Main

Jackson, A. (1997) Time-dependency of geostrophic core surface motions. Phys. Earth Planet. Int., 103, 293–311

Jault, D., Gire, C. and Le Mouël, J.-L. (1988) Westward drift, core motions and exchanges of angular momentum between core and mantle. Nature, 333, 353–356

Jochmann, H. (2003) Period variations of the Chandler wobble. J. Geodesy, 77, 454–458

Kalnay, E., Kanamitsu, M., Kistler, R., Collins, W., Deaven, D., Gandin, L., Iredell, M., Saha, S., White, G., Wollen, J., Zhu, Y., Chelliah, M., Ebisuzaki, W., Higgins, W., Janowiak, J., Mo, K.C., Ropelewski, C., Wang, J., Leetmaa, A., Reynolds, R., Jenne, R. and Joseph, D. (1996) The NMC/NCAR 40-year reanalysis project. Bull. Am. Meteor. Soc., 77, 437–471

Kaplan, G.H. (2005) The IAU resolutions on astronomical reference systems, time scales, and Earth rotation models, Techn. Ber. Circular 179, United States Naval Observatory, Washington

Kosek, W., McCarthy, D.D. and Luzum, B. (2001) El Niño impact on polar motion prediction errors. Studia Geophysica et Geodaetica, 45, 347–361

Kuehne, J., Wilson, C.R. and Johnson, S. (1996) Estimates of the Chandler wobble frequency and Q. J. Geophys. Res., 101, 13573–13580

Kusche, J. and Schrama, E. (2005) Surface mass redistribution inversion from global GPS deformation and Gravity Recovery and Climate Experiment (GRACE) gravity data. J. Geophys. Res., 110, 10.1029/2004JB003556

Lambeck, K. (1980) The Earth's Variable Rotation: Geophysical Causes and Consequences. Cambridge University Press, Cambridge

Lenhardt, H. and Groten, E. (1985) Chandler wobble parameters from BIH and ILS data. Manuscripta Geodaetica, 10, 296–305

Liao, D.C. and Greiner-Mai, H. (1999) A new ΔLOD series in monthly intervals (1892.0–1997.0) and its comparison with other geophysical results. J. Geodesy, 73, 466–477

Lieske, J.H., Lederle, T., Fricke, W. and Morando, B. (1977) Expression for the precession quantities based upon the IAU (1976) system of astronomical constants. Astron. Astrophys., 58, 1–16

Ma, C., Arias, E.F., Eubanks, T.M., Fey, A.L., Gontier, A.-M., Jacobs, C.S., Sovers, O.J., Archinal, B.A. and Charlot, P. (1998) The International Celestial Reference Frame as realized by Very Long Baseline Interferometry. Astron. J., 116, 516–546

Manabe, S., Sato, T., Sakai, S. and Yokoyama, K. (1991) Atmospheric loading effects on VLBI observations. Proceedings of the AGU Chapman Conference on Geodetic VLBI, NOAA Technical Report NOS 137 NGS 49, Rockville, pp. 111–122

Marchenko, A.N. and Schwintzer, P. (2003) Estimation of the Earth's tensor of inertia from recent global gravity field solutions. J. Geodesy, 76, 495–509

Mathews, P.M., Buffet, B.A., Herring, T.A. and Shapiro, I.I. (1991) Forced nutations of the Earth: influences of inner core dynamics, part 2: numerical results and comparisons. J. Geophys. Res., 96, 8243–8257

Mathews, P.M., Herring, T.A. and Buffet, B.A. (2002) Modeling of nutation and precession: new nutation series for nonrigid Earth and insights into the Earth's interior. J. Geophys. Res., 107, 10.1029/2001JB000390

Mendes Cerveira, P.J., Boehm, J., Schuh, H., Klügel, T., Velikoseltsev, A., Schreiber, U. and Brzezinski, A. (2009) Earth rotation observed by Very Long Baseline Interferometry and ring laser. Pure Appl. Geophys., 166, 1499–1517

McCarthy, D.D. and Capitaine, N. (2002) Practical Consequences of Resolution B1.6 'IAU2000 Precession-Nutation Model', Resolution B1.7 'Definition of Celestial Intermediate Pole', Resolution B1.8 'Definition and Use of Celestial and Terrestrial Ephemeris Origin'. In: Capitatine, N., Gambis, D., McCarthy, D.D., Petit, G., Ray, J., Richter, B., Rothacher, M., Standish, E.M. and Vondrak, J. (eds) Proceedings of the IERS Workshop on the Implementation of the New IAU Resolutions, IERS Technical Note 29, Verlag des Bundesamts für Kartographie und Geodäsie, Frankfurt am Main, pp. 9–17

McCarthy, D.D. and Petit, G. (eds) (2004) IERS Conventions 2003, IERS Technical Note 32, Verlag des Bundesamts für Kartographie und Geodäsie, Frankfurt am Main

McClure, P. (1973) Diurnal polar motion, Techn. Ber. GSFC Rep. X-529-73-259, Goddard Space Flight Cent., Greenbelt

Milly, P.C. and Shmakin, A.B. (2002) Global modeling of land water and energy balances. Part I: the land dynamics (LaD) model. J. Hydrometeorol., 3(3), 283–299

Milne, G.A. and Mitrovica, J.X. (1998) Postglacial sea-level change on a rotating Earth. Geophys. J. Int., 133, 1–19

Molodensky, M.S. (1961) The theory of nutation and diurnal Earth tides. Comm. Obs. R. Belgique, 142, 25–56

Moritz, H. and Mueller, I.I. (1987) Earth rotation. Theory and Observation. Ungar, New York

Morrison, L.V. and Stephenson, F.R. (1998) The sands of time and tidal friction. In: Brosche, P., Dick, W.R., Schwarz, O. and Wielen, R. (eds) The Message of the Angles – Astrometry from 1798 to 1998, Thun-Verlag, Frankfurt am Main, pp. 100–113

Munk, W.H. and MacDonald, G.J.F. (1960) The Rotation of the Earth. A Geophysical Discussion. Cambridge University Press, Cambridge

Okubo, S. (1982) Is the Chandler period variable? Geophys. J. R. Astr. Soc., 71, 629–646

Ponsar, S., Dehant, V., Holme, R., Jault, D., Pais, A. and Hoolst, T.V. (2002) The core and fluctuations in the Earth's rotation. In: Dehant, V., Creager, K.C., Karato, S. and Zatman, S. (eds) Earth's Core: Dynamics, Structure, Rotation. Geodynamics Series 31, American Geophysical Union, Washington, pp. 251–261

Rabbel, W. and Schuh, H. (1986) The influence of atmospheric loading on VLBI experiments. J. Geophys., 59, 164–170

Rabbel, W. and Zschau, J. (1985) Static deformations and gravity changes at the Earth's surface due to atmospheric loading. J. Geophys., 56, 81–99

Ramillien, G., Frappart, F., Cazenave, A. and Güntner, A. (2005) Time variations of land water storage from an inversion of 2 years of GRACE geoids. Earth Planet. Sci. Lett., 235, 283–301

Ray, J.R. (1996) Measurements of length of day using the Global Positioning System. J. Geophys. Res., 101, 20141–20149

Richter, B. (1995) Die Parametrisierung der Erdorientierung, Zeitschrift f. Vermessungswesen, 102(3), 109–119 (in German)

Rochester, M.G. and Smylie, D.E. (1974) On changes in the trace of the Earth's inertia tensor. J. Geophys. Res., 79, 4948–4951

Rosen, R.D., Salstein, D.A., Eubanks, T.M., Dickey, J.O. and Steppe, J.A. (1984) An El Nino signal in atmospheric angular momentum and Earth rotation. Science, 225, 411–414

Rothacher, M. (2002) Future IERS products: Implementation of the IAU 2000 Resolutions. In: Capitatine, N., Gambis, D., McCarthy, D.D., Petit, G., Ray, J., Richter, B., Rothacher, M., Standish, E.M. and Vondrak, J. (eds) Proceedings of the IERS Workshop on the Implementation of the New IAU Resolutions, IERS Technical Note 29, Verlag des Bundesamts für Kartographie und Geodäsie, Frankfurt am Main, pp. 77–84

Sasao, T., Okubo, S. and Saito, M. (1980) A simple theory on the dynamical effects of a stratified fluid core upon nutational motion of the Earth. In: Fedorov, E.P., Smith, M.L. and Bender, P.L. (eds) Nutation and the Earth's Rotation. IAU Symposia 78, D. Reidel, Kiev, pp. 165–183

Scherneck, H.G. (1990) Loading Green's functions for a continental shield with a Q-structure for the mantle and density constraints from the geoid. Bull. d'Inform. Marées Terr., 108, 7775–7792

Schneider, M. (1988) Satellitengeodäsie, BI Wissenschaftsverlag, Zürich (in German)

Schödlbauer, A. (2000) Geodätische Astronomie: Grundlagen und Konzepte, de Gruyter, Berlin (in German)

Schreiber, U., Velikoseltsev, A., Rothacher, M., Klügel, T., Stedman, G. and Wiltshire, D. (2004) Direct measurement of diurnal polar motion by ring laser gyroscopes. J. Geophys. Res., 109, 10.1029/2003JB002803

Schuh, H., Dill, R., Greiner-Mai, H., Kutterer, H., Müller, J., Nothnagel, A., Richter, B., Rothacher, M., Schreiber, U. and Soffe, M. (eds) (2003) Erdrotation und globale dynamische Prozesse,

Mitteilungen des Bundesamts für Kartographie und Geodäsie, Band 32, Verlag des Bundesamts für Kartographie und Geodäsie, Frankfurt am Main (in German)
Schuh, H., Estermann, G., Crétaux, J.-F., Bergé-Nguyen, M. and van Dam, T. (2004) Investigation of hydrological and atmospheric loading by space geodetic techniques. In: Hwang, C., Shum, C.K. and Li, J.C. (eds) Satellite Altimetry for Geodesy, Geophysics and Oceanography. IAG Symposia 126, Springer, Berlin, pp. 123–132
Schuh, H., Nagel, S. and Seitz, T. (2001) Linear drift and periodic variations observed in long time series of polar motion. J. Geodesy, 74, 701–710
Seidelmann, P.K. (ed) (1992) Explanatory Supplement to the Astronomical Almanac. University Science Books, Mill Valley
Seitz, F. (2004) Atmosphärische und ozeanische Einflüsse auf die Rotation der Erde – Numerische Untersuchungen mit einem dynamischen Erdsystemmodell, C 578, Deutsche Geodätische Kommission, München (in German)
Seitz, M. (2009) Kombination geodätischer Raumbeobachtungsverfahren zur Realisierung eines terrestrischen Referenzsystems, C 630, Deutsche Geodätische Kommission, München (in German)
Seitz, F. and Kutterer, H. (2005) Sensitivity analysis of the non-linear Liouville equation. In Sansò, F. (ed) A Window on the Future of Geodesy. IAG Symposia 128, Springer, Berlin, pp. 601–606
Seitz, F. and Schmidt, M. (2005) Atmospheric and oceanic contributions to Chandler wobble excitation determined by wavelet filtering. J. Geophys. Res., 110, 10.1029/2005JB003826
Seitz, F., Stuck, J. and Thomas, M. (2004) Consistent atmospheric and oceanic excitation of the Earth's free polar motion. Geophys. J. Int., 157, 25–35
Sidorenkov, N.S. (1992) Excitation mechanisms of Chandler polar motion. Astr. Zh., 69(4), 905–909
Smith, M.L. and Dahlen, F.A. (1981) The period and Q of the Chandler wobble. Geophys. J. R. Astr. Soc., 64, 223–281
Souchay, J., Loysel, B., Kinoshita, H. and Folgueira, M. (1999) Corrections and new developments in rigid Earth nutation theory. Final tables 'REN-200' including crossed-nutation and spin-orbit coupling effects. Astron. Astrophys. Suppl. Ser., 135, 111–131
Souriau, A. and Cazenave, A. (1985) Reevaluation of the seismic excitation of the Chandler wobble from recent data. Earth Plan. Sci. Lett., 75, 410–416
Standish, E.M. (1998) JPL planetary and lunar ephemerides DE405/LE405, Techn. Ber. IOM 312.F-98-048, JPL, Pasadena
Stuck, J. (2002) Die simulierte axiale atmosphärische Drehimpulsbilanz des ECHAM3-T21 GCM, Bonner Meteorologische Abhandlungen 56, Asgard-Verlag, Sankt Augustin (in German)
Sun, H.P., Ducarme, B. and Dehant, V. (1995) Effect of the atmospheric pressure on surface displacements. J. Geodesy, 70, 131–139
Tisserand, F. (1891) Traité de Méchanique Céleste, Vol. II. Gauthier-Villars, Paris (in French)
Torge, W. (2001) Geodesy. de Gruyter, Berlin
Trenberth, K.E. (1980) Atmospheric quasibiennial oscillations. Mon. Weather Rev., 108, 1370–1377
van Dam, T.M. and Herring, T.A. (1994) Detection of atmospheric pressure loading using very long baseline interferometry measurements. J. Geophys. Res., 99, 4505–4517
van Dam, T.M., Wahr, J., Chao, Y. and Leuliette, E. (1997) Predictions of crustal deformation and of geoid and sea level variability caused by oceanic and atmospheric loading. Geophys. J. Int., 99, 507–515
van Dam, T.M., Wahr, J., Milly, P.C.D., Shmakin, A.B., Blewitt, G., Lavalee, D. and Larson, K.M. (2001) Crustal displacements due to continental water loading. Geophys. Res. Lett., 28, 651–654
Vondrak, J., Ron, C., Pesek, I. and Cepek, A. (1995) New global solution of Earth orientation parameters from optical astrometry in 1900–1990. Astron. Astrophys., 297, 899–906
Vondrak, J., Weber, R. and Ron, C. (2005) Free core nutation: direct observations and resonance effects. Astron. Astrophys., 444, 297–303

Wahr, J.M. (1981) The forced nutations of an elliptical, rotating, elastic and oceanless Earth. Geophys. J. R. Astr. Soc., 64, 705–727
Wahr, J.M. (1982) The effects of the atmosphere and oceans on the Earth's wobble – I. Theory. Geophys. J. R. Astr. Soc., 70, 349–372
Wahr, J.M. (1983) The effects of the atmosphere and the oceans on the Earth's wobble and on the seasonal variations in the length of day – II. Results. Geophys. J. R. Astr. Soc., 74, 451–487
Wahr, J.M. (1985) Deformation induced by polar motion. J. Geophys. Res., 90, 9363–9368
Wilson, C.R. and Haubrich, R.A. (1976) Meteorological excitation of the Earth's wobble. Geophys. J. R. Astr. Soc., 46, 707–743
Wilson, C.R. and Vicente, R.O. (1990) Maximum likelihood estimates of polar motion parameters. In: McCarthy, D.D. and Carter, W.E. (eds) Variations in Earth Rotation. Geophysical Monograph Series 59, American Geophysical Union, Washington, pp. 151–155
Winkelnkemper, T., Seitz, F., Min, S. and Hense, A. (2008) Simulation of historic and future atmospheric angular momentum effects on length-of-day variations with GCMs. In: Sideris, M. (ed) Observing our Changing Earth. IAG Symposia 133, Springer, Berlin, pp. 447–454
Wu, X., Heflin, M., Ivins, E., Argus, D. and Webb, F. (2003) Large-scale global surface mass variations inferred from GPS measurements of load-induced deformation. Geophys. Res. Lett., 30(14), 10.1029/2003GL017546
Wu, X., Watkins, M., Ivins, E., Kwok, R., Wang, P. and Wahr, J. (2002) Toward global inverse solutions for current and past ice ass variations: contribution of secular satellite gravity and topography change measurements. J. Geophys. Res., 107, 10.1029/2001JB000543
Yoder, C.F., Williams, J.G. and Parke, M.E. (1981) Tidal variations of Earth rotation. J. Geophys. Res., 86, 881–891